Goal-Oriented Error Estimation for Cahn–Hilliard Models of Binary Phase Transition

Kristoffer G. van der Zee, J. Tinsley Oden, Serge Prudhomme, Andrea Hawkins-Daarud
Institute for Computational Engineering and Sciences, The University of Texas at Austin, Austin, Texas 78712

Received 28 June 2010; accepted 12 July 2010
Published online 27 October 2010 in Wiley Online Library (wileyonlinelibrary.com).
DOI 10.1002/num.20638

A posteriori estimates of errors in quantities of interest are developed for the nonlinear system of evolution equations embodied in the Cahn–Hilliard model of binary phase transition. These involve the analysis of wellposedness of dual backward-in-time problems and the calculation of residuals. Mixed finite element approximations are developed and used to deliver numerical solutions of representative problems in one- and two-dimensional domains. Estimated errors are shown to be quite accurate in these numerical examples.
 Numer Methods Partial Differential Eq 27: 160–196, 2011

Keywords: a posteriori error estimation; Cahn–Hilliard; diffuse interface; dual Cahn–Hilliard; dual well-posedness; error–residual equivalence; goal-oriented error analysis; linearized adjoint; quantities of interest

I. INTRODUCTION

The celebrated Cahn–Hilliard model of binary phase transition has generated significant interest since its inception over half a century ago [1], providing the canonical example of phase-field or diffuse-interface models of multiphase phenomena and, thereby, yielding a powerful methodology for treating complex interactions between different phases of materials [2–6]. An extensive literature exists on mathematical properties of initial-boundary-value problems driven by the Cahn–Hilliard equation and on various methods proposed for their numerical solution.

The Cahn–Hilliard equation is a fourth-order, nonlinear parabolic partial differential equation corresponding to a conservative gradient flow. Mathematical analyses of wellposedness of the Cahn–Hilliard equation were contributed by Elliott and Zheng [7], Elliott [8], Blowey and Elliott [9], Elliott and Luckhaus [10], Elliott and Garcke [11], and Barrett and Blowey [12]. Many aspects of the Cahn–Hilliard equation have been explored, for example, its dynamical properties [13] as well as its limit to certain free-boundary problems [14–16]. For a recent investigation of linear instability, we refer to Burger et al. [17].

Correspondence to: J. Tinsley Oden, Institute for Computational Engineering and Sciences, The University of Texas at Austin, 1 University Station, CO200, Austin, TX 78712 (e-mail: oden@ices.utexas.edu)
Contract grant sponsor: DOE Multiscale Mathematics; contract grant number: DE-FG02-05ER25701
Contract grant sponsor: KAUST; contract grant number: US00003

Semi-discrete (discrete in space, continuous in time) approximations of the Cahn–Hilliard equation lead to very stiff ordinary differential equations that provide a challenge for most implicit numerical schemes and are generally intractable by explicit methods. The development of so-called semi-implicit time-stepping algorithms is an ongoing area of research; see Eyre [18], He, Liu and Tang [19], and He and Liu [20] (cf. Feng and Prohl [21]), as well as algorithms developed for related equations in [22, 23]. Finite element approximations of the Cahn–Hilliard equation have been analyzed in a series of papers by Elliott and French [24], Copetti and Elliott [25], Barrett and Blowey [12, 26], and Feng and Prohl [27]. The latest of these developments considered discontinuous Galerkin methods [28–30] and isogeometric methods [31].

The subject of a posteriori error estimates and adaptive methods for finite element approximations of the Cahn–Hilliard equation has recently been taken up by Feng and Wu [32], and Bartels and Müller [33]; see also the applications to the Cahn–Hilliard equation with a double obstacle free energy in [34, 35], and to the Allen–Cahn equation in [36–38]. One of the main focuses in [32, 36, 38] in developing these estimates is the elimination of their exponential dependence on the interface thickness parameter ϵ. This elimination is possible when the solution exhibits developed layers without undergoing topological changes but appears unavoidable in the general case. The estimates developed in [33, 37], on the other hand, explicitly monitor and take into account such topological changes by computing an approximation to the principal eigenvalue of the linearized operator.

In this work, we develop goal-oriented error estimates for the Cahn–Hilliard equation. These error estimates are dual-based a posteriori estimates of the error in output functionals of the solution. The estimates are applicable to general classes of Cahn–Hilliard initial value problems, and do not rely on developed layers, since the precise influence of the residual on the error is provided by the dual solution, which is the solution of a backward-in-time, linearized-adjoint problem.

The idea of goal-oriented methods embraces the notion that a numerical simulation is generally done to study specific features of the solutions, the so-called quantities of interest or target outputs, which are, therefore, the goals of the analyses. Obviously, it is important to be able to estimate the discretization error in such quantities of interest, and, once an estimate is in hand, to adapt the mesh so as to control the error. This is the mission of goal-oriented adaptive finite element methods. The theory of a posteriori error estimation was confined to global estimates in various energy and L^p-norms until the late 1990s, when the idea of using adjoints (duals) to arrive at estimates of quantities of interest emerged. Such estimates are presented in the works of Oden and Prudhomme [39–42], the important works of Becker and Rannacher [43, 44] (see also [45]), Süli and Houston [46, 47], and Paraschivoiu et al. [48] (see also [49]).

The application of goal-oriented methods to time-dependent problems poses a significant complication as it requires a computation of the global backward-in-time dual problem. Various implementations of such algorithms have been investigated by Bangerth and Rannacher [50], Fuentes et al. [51], Díez and Calderón [52], Schmich and Vexler [53], Bermejo and Carpio [54], and Carey et al. [55]. In the present exposition, we describe the extension of time-dependent goal-oriented methods to the nonlinear Cahn–Hilliard equation.

We note that goal-oriented error estimates for time-dependent problems are similar in their derivation to the dual-based error estimates developed for parabolic equations by Eriksson and Johnson in a series of papers in the 1990s [56–59]; see also [60, 61]. However, the focus of their work is on a global norm of the error, and the influence of the dual problem in the estimates is reduced to a proportionality factor, the so-called stability constant.

Following this introduction, we present the initial-boundary-value-problem on polyhedral domains in $\mathbb{R}^d$, governed by the Cahn–Hilliard equation. We develop a weak mixed variational formulation of this problem for the pair (u, μ), u being a species or phase concentration and μ

the chemical potential. We then consider semi-discrete and fully-discrete mixed finite element approximations of the system using equal-order polynomial approximations of (u, μ) in space and globally continuous approximations in time. In Section III, we develop global bounds on the error components $e^u = u - \hat{u}$, $e^\mu = \mu - \hat{\mu}$, $(\hat{u}, \hat{\mu})$ being any pair satisfying mild compatibility conditions, in terms of the residual functionals for the system. The development of a posteriori estimates of error in quantities of interest is taken up in Section IV. For simplicity, we choose to define these quantities of interest through continuous linear functionals on the space of trial functions, but the theory captures cases involving nonlinear, differentiable functionals. We derive backward-in-time dual (or linearized-adjoint) equations, the well posedness of which is shown in Section V. The solution pair (p, χ) of the dual problem is then used to derive goal-oriented error estimates in quantities of interest. In Section VI, we develop numerical algorithms for computing the goal-oriented error estimates and we present results of several numerical experiments on one- and two-dimensional examples that confirm the predictions of the theory.

II. PROBLEM STATEMENT

A. The Cahn–Hilliard Model

Let $\Omega \subset \mathbb{R}^d$, $d = 1, 2, 3$, be a bounded (polyhedral for $d = 2, 3$) domain. We consider the following nonlinear initial boundary-value problem for the pair (u, μ):

$$\left.\begin{aligned} u_t &= \Delta\mu \\ \mu &= \psi'(u) - \epsilon^2\,\Delta u \end{aligned}\right\} \quad \text{in } \Omega \times (0, T]\,, \tag{1a}$$

$$\partial_n u = \partial_n \mu = 0 \quad \text{on } \partial\Omega \times [0, T]\,, \tag{1b}$$

$$u = u_0 \quad \text{on } \Omega \times \{t = 0\}\,, \tag{1c}$$

where $(\cdot)_t = \partial_t(\cdot) = \partial(\cdot)/\partial t$, $\partial_n(\cdot) = n \cdot \nabla(\cdot)$ is the normal derivative, ϵ^2 the diffusivity, $\psi : \mathbb{R} \to \mathbb{R}$ the free energy, and $u_0 \in H^1(\Omega)$ is an initial condition. Physically interesting cases concern small diffusivity, i.e., $\epsilon^2 \leq 1$.

The nonlinear free energy function ψ has the form of a double well. This form provides the mechanism for phase separation. We shall consider the following C^2-continuous double well ψ:

$$\psi(u) := \begin{cases} (u+1)^2 & u < -1, \\ \dfrac{1}{4}(u^2-1)^2 & u \in [-1, 1], \\ (u-1)^2 & u > 1. \end{cases} \tag{2}$$

In particular, we shall employ the following important properties of ψ:

$$(\psi'(u) - \psi'(v))(u - v) \geq -C_1(u - v)^2, \quad \forall u, v \in \mathbb{R}. \tag{3a}$$

$$|\psi'(u) - \psi'(v)| \leq L_{\psi'}|u - v|, \quad \forall u, v \in \mathbb{R}, \tag{3b}$$

$$|\psi''(u) - \psi''(v)| \leq L_{\psi''}|u - v|, \quad \forall u, v \in \mathbb{R}, \tag{3c}$$

for positive constants C_1, $L_{\psi'}$, and $L_{\psi''}$, in particular, $6C_1 = 3L_{\psi'} = L_{\psi''} = 6$. These properties correspond to compact perturbations of monotonicity (or a Gårding inequality), Lipschitz continuity of ψ' and Lipschitz continuity of ψ'', respectively.

Remark 2.1. Note that we consider a modification of the classical quartic free energy, $\frac{1}{4}(u^2-1)^2$. This modification is such that ψ has quadratic tails, implying that ψ' has linear growth at infinity. Such assumptions have been employed in, e.g., [62] to derive L^∞-bounds for u. Our motivation is that we can establish well posedness of dual Cahn–Hilliard problems; see Section V.

A different free energy that satisfies the properties (3a)–(3c) is the regularized logarithmic free energy [12, 26]:

$$\psi_\delta(u) := \begin{cases} \frac{\theta_c}{2}(1-u^2) + \frac{\theta}{2}\Big((1-u)\ln\frac{1-u}{2} \\ \qquad + \frac{1}{2\delta}(1+u)^2 + (1+u)\ln\frac{\delta}{2} - \frac{\delta}{2}\Big) & u < -1+\delta, \\ \frac{\theta_c}{2}(1-u^2) + \frac{\theta}{2}\Big((1+u)\ln\frac{1+u}{2} + (1-u)\ln\frac{1-u}{2}\Big) & u \in [-1+\delta, 1-\delta], \\ \frac{\theta_c}{2}(1-u^2) + \frac{\theta}{2}\Big((1+u)\ln\frac{1+u}{2} \\ \qquad + \frac{1}{2\delta}(1-u)^2 + (1-u)\ln\frac{\delta}{2} - \frac{\delta}{2}\Big) & u > 1-\delta. \end{cases}$$

where θ and $\theta_c > \theta$ are positive constants and $\delta > 0$ is a small number. Furthermore, the regularized double obstacle free energy (corresponding to a deep quench limit) in [9] also satisfies these properties.

Remark 2.2. The Cahn–Hilliard equation is a conservative gradient flow equation [63]. It is conservative as it preserves mass,

$$\int_\Omega u(t)\,\mathrm{d}x = \int_\Omega u_0\,\mathrm{d}x, \qquad \forall t \in [0,T]. \tag{4}$$

It is a gradient flow, since one can show that $u_t = \Delta(\delta_u\mathcal{E}(u))$, where $\delta_u\mathcal{E}(u)$ is the Gâteaux (or Fréchet) differential (in $L^2(\Omega)$) of the total free energy,[1]

$$\mathcal{E}(u) := \int_\Omega \left(\psi(u) + \frac{\epsilon^2}{2}|\nabla u|^2\right)\mathrm{d}x.$$

An important consequence is that the total energy satisfies

$$\frac{\mathrm{d}}{\mathrm{d}t}\mathcal{E}(u(t)) = -\int_\Omega |\nabla\mu(t)|^2\,\mathrm{d}x, \tag{5}$$

that is, the energy decreases monotonically as $t \to +\infty$.

B. Weak Formulation

We consider a mixed weak formulation of (1), i.e., a weak formulation involving both u and μ as separate unknowns. To provide a proper functional setting, we first recall the following preliminaries specific for time-dependent problems; for more details, see e.g., [64, Section 5.9 and Chapter 7] or [65, Chapter 18].

[1]More precisely, it is shown in [63] that $u_t = -\delta_u\mathcal{E}(u)$, with $\delta_u\mathcal{E}(u)$ the Gâteaux (or Fréchet) differential in the space $\mathcal{H}'$, $\mathcal{H}'$ being the zero-average subspace of $H^1(\Omega)'$ defined in Section III B.

We define the following Hilbert space consisting of functions of time $t \in (0,T)$ with values in $H^1(\Omega)$ and corresponding norm:

$$\mathcal{V} := L^2(0,T;H^1(\Omega)), \quad \|v\|_{\mathcal{V}}^2 := \int_0^T \|v(t)\|_{H^1(\Omega)}^2 \,\mathrm{d}t.$$

The space $\mathcal{V}$ shall be a suitable space for μ. As a suitable space for u, we define

$$\mathcal{W} := \{v \in \mathcal{V} \,:\, v_t \in \mathcal{V}' := L^2(0,T;H^1(\Omega)')\},$$

for which the norm is defined as

$$\|v\|_{\mathcal{W}}^2 := \|v\|_{\mathcal{V}}^2 + \|v_t\|_{\mathcal{V}'}^2,$$

where

$$\|v_t\|_{\mathcal{V}'}^2 := \int_0^T \|v_t(t)\|_{H^1(\Omega)'}^2 \,\mathrm{d}t,$$

and the $H^1(\Omega)$ dual norm is defined as[2]

$$\|\cdot\|_{H^1(\Omega)'} := \sup_{w \in H^1(\Omega)} \frac{\langle \cdot, w\rangle}{\|w\|_{H^1(\Omega)}},$$

$\langle\cdot,\cdot\rangle$ denoting a suitable duality pairing. Note that $\mathcal{W} \subset \mathcal{V}$. For $v \in \mathcal{W}$, we have that $v \in C([0,T];L^2(\Omega))$ by a classical embedding result [65, p. 473]. Then, for $v, w \in \mathcal{W}$, the integration by parts formula holds:

$$\int_0^T \big\langle w_t(t), v(t)\big\rangle \,\mathrm{d}t = (w(T), v(T)) - (w(0), v(0)) - \int_0^T \big\langle v_t(t), w(t)\big\rangle \,\mathrm{d}t, \tag{6}$$

where $(\cdot,\cdot)$ denotes the $L^2(\Omega)$-inner product with associated norm denoted simply by $\|\cdot\|$. Furthermore, we can enforce strongly the initial condition for u, and set

$$\mathcal{W}_{u_0} := \{v \in \mathcal{W} : v(0) = u_0\}.$$

The weak formulation of (1) is now defined as

$$\boxed{\begin{aligned} &\text{Find } (u,\mu) \in \mathcal{W}_{u_0} \times \mathcal{V}: \\ &\qquad\qquad \big\langle u_t(t), v\big\rangle + \big(\nabla\mu(t), \nabla v\big) = 0 \qquad \forall v \in H^1(\Omega)\,, \qquad (7a)\\ &-\epsilon^2\big(\nabla u(t), \nabla\eta\big) + \big(-\psi'(u(t)) + \mu(t), \eta\big) = 0 \qquad \forall \eta \in H^1(\Omega)\,, \qquad (7b)\\ &\qquad\qquad\qquad\qquad\qquad\qquad \text{a.e. } 0 \le t \le T\,. \end{aligned}}$$

[2]In this article, we abuse the inf and sup notation for fractions by writing, for example, $\sup_{w\in H^1(\Omega)} \frac{\langle\cdot,w\rangle}{\|w\|_{H^1(\Omega)}}$ instead of $\sup_{w\in H^1(\Omega)\setminus\{0\}} \frac{\langle\cdot,w\rangle}{\|w\|_{H^1(\Omega)}}$.

It is known that there exists a unique weak solution to (7); see, e.g., [8,9,11,26] for various proofs. Moreover, the following a priori estimate holds:

$$\epsilon^2 \|u\|^2_{L^\infty(0,T;H^1(\Omega))} + \|u_t\|^2_{\mathcal{V}'} + \|\mu\|^2_{\mathcal{V}} \leq C, \tag{8}$$

where $\|u\|_{L^\infty(0,T;H^1(\Omega))} := \sup_{t\in[0,T]} \|u(t)\|_{H^1(\Omega)}$ and the constant C depends on Ω, T, and $\|u_0\|_{H^1(\Omega)}$.

C. Approximations

We shall consider approximations to the Cahn–Hilliard equation based on discretizing the mixed weak formulation (7) separately in space and time.

In space, we consider conforming Galerkin discretizations employing so-called Ciarlet–Raviart (equal-order) mixed finite elements [66, 67]. Let $\mathcal{P}^h$ denote a conformal partition $\mathcal{P}^h$ of Ω into nonoverlapping elements K such that $\bar{\Omega} = \cup_{K\in\mathcal{P}^h} \bar{K}$. Each element is the image of an invertible, generally affine map F_K of a master or reference element $\hat{K}$. Let $P^r(\hat{K})$ denote the space of complete polynomials of degree $\leq r$ on $\hat{K}$, and let $Q^r(\hat{K})$ denote the space of tensor products of polynomials of degree $\leq r$ on $\hat{K}$. Then, we introduce the finite-dimensional spaces S^h of conforming finite elements defined by

$$S^h := S^{h,r}(\mathcal{P}^h) := \left\{ v^h \in H^1(\Omega) \,:\, v^h|_K = \hat{v} \circ F_K^{-1}\,,\ \hat{v} \in P^r(\hat{K}) \text{ or } \in Q^r(\hat{K})\,,\ \forall K \in \mathcal{P}^h \right\}.$$

Accordingly, the semi-discrete, time-continuous, space-discrete approximation (u^h, μ^h) : $[0, T] \to S^h$ is defined by

$$(u^h_t(t), v) + (\nabla\mu^h(t), \nabla v) = 0 \qquad \forall v \in S^h\,, \tag{9a}$$

$$-\epsilon^2\,(\nabla u^h(t), \nabla\eta) + \big(-\psi'(u^h(t)) + \mu^h(t), \eta\big) = 0 \qquad \forall \eta \in S^h\,, \tag{9b}$$

$$\text{a.e. } 0 \leq t \leq T$$

together with the initial condition

$$(u^h(0), w) = (u_0, w) \quad \forall w \in S^h. \tag{9c}$$

We consider full discretizations by applying a time-integration method to (9). Let $0 = t^0 < t^1 < \cdots < t^N = T$, $N \geq 1$, denote a sequence of discrete time steps partitioning $[0, T]$ into time intervals $(t^{n-1}, t^n]$ of length $\Delta t^n := t^n - t^{n-1}$, $n = 1, \ldots, N$. In this work, we shall focus on fully conforming approximations $(\hat{u}, \hat{\mu})$ in the sense that $(\hat{u}, \hat{\mu}) \in \mathcal{W} \times \mathcal{V}$. This can be achieved by a continuous Galerkin-in-time method or by a time-marching algorithm if the solution at the discrete time levels $\{t^n\}$ is appropriately interpolated or reconstructed. We refer to Section VI for an example of the latter. The reason for considering conforming approximations is that it allows us to evaluate the residual functionals associated with (7).[3] We thus consider approximations

$$(\hat{u}, \hat{\mu}) \in \hat{\mathcal{W}} \times \hat{\mathcal{V}} \subset \mathcal{W} \times \mathcal{V},$$

[3]Extensions to discontinuous Galerkin-in-time of piecewise-continuous-in-time reconstructions are possible provided one takes into account the jumps of $\hat{u}$ at each time step.

where

$$\hat{\mathcal{V}} := \hat{\mathcal{V}}^{h,\Delta t} := \{\hat{v} \in \mathcal{V} \,:\, \hat{v}|_{(t^{n-1},t^n]} \in C^0((t^{n-1},t^n];S^h)\,,\ \forall n = 1,\dots,N\},$$
$$\hat{\mathcal{W}} := \hat{\mathcal{W}}^{h,\Delta t} := \{\hat{v} \in \mathcal{W} \,:\, \hat{v} \in C^0([0,T];S^h)\,,\ \hat{v}_t \in \hat{\mathcal{V}}^{h,\Delta t}\},$$

A remarkable fact is that, in most of the ensuing analysis, it is not necessary that the approximations be obtained by the above discretization scheme. All that is required is for the approximations to be conforming. To simplify some of the analysis, we shall, however, assume that approximations preserve mass exactly:

$$\int_\Omega \hat{u}(t)\,\mathrm{d}x = \int_\Omega u_0\,\mathrm{d}x, \quad t \in [0,T]. \tag{10}$$

On account of (4), this implies that the error in the average of u vanishes:

$$⨍(u - \hat{u})(t) = 0, \tag{11}$$

where we introduce the average symbol $⨍(\cdot) := \int_\Omega(\cdot)\mathrm{d}x/|\Omega|$. We note that the mass conservation assumption (10) is not restrictive. In particular, for the semidiscrete approximation u^h, it is implied by (9a) (with $v = 1$) and (9c) (with $w = 1$). Moreover, it is satisfied by fully discrete approximations based on Galerkin-in-time discretizations or suitably reconstructed time-stepping algorithms with the condition $⨍\,\hat{u}(0) = ⨍\,u_0$.

III. ERROR–RESIDUAL EQUIVALENCE

In goal-oriented error analysis, the error in the quantity of interest is related to the residuals weighted by an appropriate dual solution. The relevant residuals are defined as[4]

$$\hat{\mathcal{R}}_1(v) := \mathcal{R}_1((\hat{u}(t),\hat{\mu}(t));v) := -\langle \hat{u}_t(t), v\rangle - (\nabla\hat{\mu}(t),\nabla v), \tag{12a}$$

$$\hat{\mathcal{R}}_2(\eta) := \mathcal{R}_2((\hat{u}(t),\hat{\mu}(t));\eta) := -(\hat{\mu}(t) - \psi'(\hat{u}(t)),\eta) + \epsilon^2(\nabla\hat{u}(t),\nabla\eta), \tag{12b}$$

$$\hat{\mathcal{R}}_{\mathrm{IC}}(w) := \mathcal{R}_{\mathrm{IC}}(\hat{u}(0);w) := (u_0 - \hat{u}(0), w), \tag{12c}$$

for $v,\eta \in H^1(\Omega)$, and $w \in L^2(\Omega)$. These residuals correspond to (7a), (7b), and the initial condition, respectively. Note that the mass conservation assumption (10) implies that

$$\hat{\mathcal{R}}_1(1) = \frac{\mathrm{d}}{\mathrm{d}t}\int_\Omega \hat{u}(t)\,\mathrm{d}x = 0, \tag{13a}$$

$$\hat{\mathcal{R}}_{\mathrm{IC}}(1) = \int_\Omega \big(\hat{u}(0) - u_0\big)\,\mathrm{d}x = 0. \tag{13b}$$

Before we consider goal-oriented error estimates, let us first show that the error is actually equivalent to the residual. This error–residual equivalence is usually studied in the context of linear steady problems, see e.g. [42]. The constants involved in the equivalence relation are typically

[4]For semilinear functionals, we use the convention that the functional is linear with respect to the arguments after the semicolon ";".

dependent on the parameters of the problem at hand, and in case of time-dependent problems, dependent on the time-interval length T.

The first step toward obtaining error–residual equivalence is to define the equations for the error:

$$\left(e^u_t, v\right) + (\nabla e^\mu, \nabla v) = \hat{\mathcal{R}}_1(v) \qquad v \in H^1(\Omega), \tag{14a}$$

$$-\epsilon^2 (\nabla e^u, \nabla \eta) + (e^\mu, \eta) - (\psi'(u) - \psi'(\hat{u}), \eta) = \hat{\mathcal{R}}_2(\eta) \qquad \eta \in H^1(\Omega), \tag{14b}$$

$$\text{a.e. } 0 \le t \le T.$$

where we used the shorthand notation

$$e^u := u - \hat{u} \quad \text{and} \quad e^\mu := \mu - \hat{\mu}.$$

A. Residual Upper Bound

An upper bound on the $H^1(\Omega)'$-norm of $\hat{\mathcal{R}}_1$ and $\hat{\mathcal{R}}_2$ can be derived by bounding the left-hand side of (14a) and (14b), respectively. It shall be convenient to separate a bound on a $H^1(\Omega)'$-norm into two distinct parts.

Let $\hat{\mathcal{R}} \in H^1(\Omega)'$, then

$$\|\hat{\mathcal{R}}\|_{H^1(\Omega)'} = \sup_{v \in H^1(\Omega)} \frac{\hat{\mathcal{R}}(v)}{\|v\|_{H^1(\Omega)}} \le \sup_{v \in H^1(\Omega)} \frac{\hat{\mathcal{R}}(⨍ v)}{\|v\|_{H^1(\Omega)}} + \sup_{v \in H^1(\Omega)} \frac{\hat{\mathcal{R}}(v - ⨍ v)}{\|v\|_{H^1(\Omega)}}. \tag{15}$$

Note that for $v \in H^1(\Omega)$, we have the decomposition $v = \mathring{v} + ⨍ v$, where $\mathring{v} := v - ⨍ v$ is a member of

$$\mathring{H}^1(\Omega) := \left\{ v \in H^1(\Omega) : ⨍ v = 0 \right\},$$

which is the subspace of functions in $H^1(\Omega)$ with zero average and corresponding norm $\|v\|_{\mathring{H}^1(\Omega)} := \|\nabla v\|$. Owing to orthogonality between $\mathring{v}$ and $⨍ v$, we have

$$\|v\|^2_{H^1(\Omega)} = \|\mathring{v}\|^2_{H^1(\Omega)} + \left\| ⨍ v \right\|^2.$$

This result implies

$$\sup_{v \in H^1(\Omega)} \frac{\hat{\mathcal{R}}(⨍ v)}{\|v\|_{H^1(\Omega)}} = \sup_{v \in H^1(\Omega)} \frac{\hat{\mathcal{R}}(⨍ v)}{\sqrt{\|\mathring{v}\|^2_{H^1(\Omega)} + \|⨍ v\|^2}} = \sup_{v \in \{1\}} \frac{\hat{\mathcal{R}}(⨍ v)}{\|⨍ v\|} = |\hat{\mathcal{R}}(1)|\, |\Omega|^{-1/2},$$

where, in the second step, we noted that the sup is attained for $\mathring{v} = 0$. Similarly, we have

$$\sup_{v \in H^1(\Omega)} \frac{\hat{\mathcal{R}}(v - ⨍ v)}{\|v\|_{H^1(\Omega)}} = \sup_{\mathring{v} \in \mathring{H}^1(\Omega)} \frac{\hat{\mathcal{R}}(\mathring{v})}{\|\mathring{v}\|_{H^1(\Omega)}} \le \sup_{\mathring{v} \in \mathring{H}^1(\Omega)} \frac{\hat{\mathcal{R}}(\mathring{v})}{\|\mathring{v}\|_{\mathring{H}^1(\Omega)}}.$$

Substituting these two results into (15), we obtain the bound

$$\boxed{\|\hat{\mathcal{R}}\|_{H^1(\Omega)'} \le C\left(|\hat{\mathcal{R}}(1)| + \|\hat{\mathcal{R}}\|_{\mathring{H}^1(\Omega)'}\right).} \tag{16}$$

Next, recall that there is a constant $C_{\mathrm{P}} > 0$ such that the Poincaré–Friedrichs inequality holds:

$$\|v\| \leq C_{\mathrm{P}} \|v\|_{\mathring{H}^1(\Omega)}, \quad \forall v \in \mathring{H}^1(\Omega). \tag{17}$$

Using this, it also follows that

$$\begin{aligned} \|\hat{\mathcal{R}}\|_{\mathring{H}^1(\Omega)'} &= \sup_{v \in \mathring{H}^1(\Omega)} \frac{\hat{\mathcal{R}}(v)}{\|v\|_{\mathring{H}^1(\Omega)}} \leq (1 + C_{\mathrm{P}}) \sup_{v \in \mathring{H}^1(\Omega)} \frac{\hat{\mathcal{R}}(v)}{\|v\|_{H^1(\Omega)}} \\ &= (1 + C_{\mathrm{P}}) \sup_{v \in H^1(\Omega)} \frac{\hat{\mathcal{R}}(v - ⨍ v)}{\|v\|_{H^1(\Omega)}}. \end{aligned} \tag{18}$$

In particular, if $\hat{\mathcal{R}}(1) = 0$, then (16) and (18) show that $\|\hat{\mathcal{R}}\|_{H^1(\Omega)'}$ and $\|\hat{\mathcal{R}}\|_{\mathring{H}^1(\Omega)}$ are equivalent. We thus have this equivalence for the first equation residual $\hat{\mathcal{R}}_1$ on account of mass conservation, see (13a), and, accordingly, need only consider functions in $\mathring{H}^1(\Omega)$ when bounding $\|\hat{\mathcal{R}}_1\|_{H^1(\Omega)'}$.

We summarize the upper bound in the following proposition.

Proposition 3.1 (residual upper bound). *Let* $(u, \mu) \in \mathcal{W}_{u_0} \times \mathcal{V}$ *denote the solution of* (7) *and* $(\hat{u}, \hat{\mu}) \in \mathcal{W} \times \mathcal{V}$ *denote any approximation satisfying mass conservation* (10). *Then the following upper bound holds:*

$$\begin{aligned} &\|\hat{\mathcal{R}}_{\mathrm{IC}}\|^2 + \int_0^T \left(\|\hat{\mathcal{R}}_1\|^2_{\mathring{H}^1(\Omega)'} + \|\hat{\mathcal{R}}_2\|^2_{H^1(\Omega)'} \right) \mathrm{d}t \\ &\qquad \leq C \left(\|e^u(0)\|^2 + \int_0^T \left(\|e^u_t\|^2_{\mathring{H}^1(\Omega)'} + \|e^u\|^2_{\mathring{H}^1(\Omega)} + \|e^\mu\|^2_{H^1(\Omega)} \right) \mathrm{d}t \right), \end{aligned} \tag{19}$$

where C *depends on* Ω *but not on* T *or* ϵ.

Proof. The proof follows by bounding the three residuals separately and adding the results. **(I)** Estimate for $\hat{\mathcal{R}}_{\mathrm{IC}}$. Note that the norm of $\hat{\mathcal{R}}_{\mathrm{IC}}$ is equal to the norm of $e^u(0)$:

$$\|\hat{\mathcal{R}}_{\mathrm{IC}}\| = \sup_{w \in L^2(\Omega)} \frac{(u_0 - \hat{u}(0), w)}{\|w\|} = \|e^u(0)\|. \tag{20}$$

(II) Bound on $\mathcal{R}_1$. Consider $v \in \mathring{H}^1(\Omega)$. The first error equation (14a) yields

$$\hat{\mathcal{R}}_1(v) = \langle e^u_t, v \rangle + (\nabla e^\mu, \nabla v) \leq \left\| e^u_t \right\|_{\mathring{H}^1(\Omega)'} \|\nabla v\| + \|\nabla e^\mu\| \|\nabla v\|,$$

so

$$\|\hat{\mathcal{R}}_1\|_{\mathring{H}^1(\Omega)'} \leq \|e^u_t\|_{\mathring{H}^1(\Omega)'} + \|\nabla e^\mu\|.$$

(III) Bound on $\mathcal{R}_2$. First consider $\eta = 1$ in the second-error equation (14b):

$$\begin{aligned} \hat{\mathcal{R}}_2(1) &= (e^\mu, 1) - (\psi'(u) - \psi'(\hat{u}), 1) \leq \|e^\mu\| \, |\Omega|^{1/2} + L_{\psi'} \, \|e^u\| \, |\Omega|^{1/2} \\ &\leq C(\|e^\mu\| + \|\nabla e^u\|), \end{aligned}$$

where we used Lipschitz continuity (3b) in the first step and the Poincaré–Friedrichs inequality (17) in the second step since $e^u \in \mathring{H}^1(\Omega)$; see (11). Next consider $\eta \in \mathring{H}^1(\Omega)$:

$$\hat{\mathcal{R}}_2(\eta) = (e^\mu, \eta) - (\psi'(u) - \psi'(\hat{u}), \eta) - \epsilon^2(\nabla e^u, \nabla\eta).$$

Before we bound the terms on the right-hand side, note that we can subtract the average of e^μ. Thus,

$$\begin{aligned}\hat{\mathcal{R}}_2(\eta) &= (e^\mu - ⨍ e^\mu, \eta) - (\psi'(u) - \psi'(\hat{u}), \eta) - \epsilon^2(\nabla e^u, \nabla\eta)\\ &\le C_{\mathrm{P}}\|\nabla e^\mu\|\|\eta\| + L_{\psi'}C_{\mathrm{P}}\|\nabla e^u\|\|\eta\| + \epsilon^2\|\nabla e^u\|\|\nabla\eta\|\\ &\le C(\|\nabla e^\mu\| + \|\nabla e^u\|)\|\nabla\eta\|.\end{aligned}$$

So, combining these results in the upper bound (16) (with $\hat{\mathcal{R}} = \hat{\mathcal{R}}_2$) yields

$$\|\hat{\mathcal{R}}_2\|_{H^1(\Omega)'} \le C(\|e^\mu\|_{H^1(\Omega)} + \|\nabla e^u\|).$$

■

B. Residual Lower Bound

Next, we would like to establish the reverse inequality. Note that this is essentially an upper bound of the error in terms of the residual, which is the key element in residual-based a posteriori error estimation, also referred to as an abstract a posteriori error estimate. The derivation of such an estimate for nonlinear problems is nontrivial. In fact, such an estimate has been established only in terms of weaker norms by Feng and Wu [32], see also [33]. Furthermore, to derive their result, Feng and Wu assume that a particular spectrum estimate holds, which is known to hold if the solution has developed layers. In this case, one is able to show the bound with a constant depending only polynomially on ϵ^{-1} instead of exponentially. In the general case, when the spectrum estimate does not hold, a bound with a constant depending exponentially on ϵ^{-1} is obtained.

Let us present the bound in the general case. The strategy is to select suitable testfunctions in the error equations (14) resulting in norms of the error on the left-hand side. The testfunctions and the measure of the error will involve the inverse Laplacian $\Delta^{-1} : \mathcal{H}' \to \mathring{H}^1(\Omega)$, where $\mathcal{H}' := \{r \in H^1(\Omega)' : \langle r, 1\rangle = 0\}$. The inverse Laplacian is defined such that

$$(\nabla(\Delta^{-1}r), \nabla\eta) = -\langle r, \eta\rangle \qquad \forall\eta \in H^1(\Omega),\ r \in \mathcal{H}'.$$

Note that for $r = v \in \mathring{H}^1(\Omega)$ and $\eta = \Delta^{-1}v$, we have $\|\nabla\Delta^{-1}v\|^2 = -(v, \Delta^{-1}v) \le \|v\|\, C_{\mathrm{P}}\|\nabla\Delta^{-1}v\|$. Thus, the following a priori estimate holds:

$$\|\Delta^{-1}v\|_{\mathring{H}^1(\Omega)} = \|\nabla\Delta^{-1}v\| \le C_{\mathrm{P}}\|v\| \le C_{\mathrm{P}}^2\|v\|_{\mathring{H}^1(\Omega)} \qquad \forall v \in \mathring{H}^1(\Omega). \tag{21}$$

Proposition 3.2 (abstract a posteriori error estimate). *Under the assumptions of Proposition 3.1, the following bound holds:*

$$\begin{aligned}&\sup_{t\in[0,T]} \|\nabla\Delta^{-1}e^u(t)\|^2 + \epsilon^2\int_0^T \left(\|\nabla e^u\|^2 + \|e^\mu\|^2_{H^1(\Omega)'}\right) \mathrm{d}t\\ &\qquad \le C\,\mathrm{e}^{T/\epsilon^2}\left(\|\hat{\mathcal{R}}_{\mathrm{IC}}\|^2 + \epsilon^{-2}\int_0^T \left(\|\hat{\mathcal{R}}_1\|^2_{\mathring{H}^1(\Omega)'} + \|\hat{\mathcal{R}}_2\|^2_{H^1(\Omega)'}\right) \mathrm{d}t\right),\end{aligned} \tag{22}$$

where C depends on Ω but not on T or ϵ.

Proof. We follow the ideas in [32]. We split the proof in two parts considering separately e^u and e^μ.

(I) Bound on e^u. Choose $v = -\Delta^{-1}e^u$ in (14a) and note that $\langle e^u_t, -\Delta^{-1}e^u\rangle = \frac{1}{2}\frac{\mathrm{d}}{\mathrm{d}t}\|\nabla\Delta^{-1}e^u\|^2$:

$$\frac{1}{2}\frac{\mathrm{d}}{\mathrm{d}t}\|\nabla\Delta^{-1}e^u\|^2 + (e^\mu, e^u) = \hat{\mathcal{R}}_1(-\Delta^{-1}e^u) \le \|\hat{\mathcal{R}}_1\|_{\mathring{H}^1(\Omega)'}\,\|\nabla\Delta^{-1}e^u\|$$
$$\le C_{\mathrm{P}}^2\|\hat{\mathcal{R}}_1\|_{\mathring{H}^1(\Omega)'}\,\|\nabla e^u\|,$$

where we used (21) in the last step as $e^u \in \mathring{H}^1(\Omega)$ (recall (11)). Next choose $\eta = -e^u$ in (14b):

$$-(e^\mu, e^u) + (\psi'(u) - \psi'(\hat{u}), e^u) + \epsilon^2\|\nabla e^u\|^2 = -\hat{\mathcal{R}}_2(e^u).$$

Using the perturbed monotonicity of ψ, see (3a), we obtain

$$-(e^\mu, e^u) + \epsilon^2\|\nabla e^u\|^2 \le C_1\|e^u\|^2 + \|\hat{\mathcal{R}}_2\|_{\mathring{H}^1(\Omega)'}\|\nabla e^u\|.$$

Adding the two results cancels the mixed (e^μ, e^u)-term and results in

$$\frac{1}{2}\frac{\mathrm{d}}{\mathrm{d}t}\|\nabla\Delta^{-1}e^u\|^2 + \epsilon^2\|\nabla e^u\|^2 \le C_1\|e^u\|^2 + C(\|\hat{\mathcal{R}}_1\|_{\mathring{H}^1(\Omega)'} + \|\hat{\mathcal{R}}_2\|_{\mathring{H}^1(\Omega)'})\|\nabla e^u\|.$$

Note that this estimate shows control of $\|\nabla\Delta^{-1}e^u\|^2$ and of $\|\nabla e^u\|^2$ but not directly of $\|e^u\|^2$. Invoking the Poincaré–Friedrichs inequality on $\|e^u\|^2$ would not help as the control of $\|\nabla e^u\|^2$ is very small (ϵ^2). Instead, we note from the definition of the inverse Laplacian:

$$\|e^u\|^2 = -(\nabla\Delta^{-1}e^u, \nabla e^u) \le \|\nabla\Delta^{-1}e^u\|\|\nabla e^u\|,$$

so that

$$\frac{1}{2}\frac{\mathrm{d}}{\mathrm{d}t}\|\nabla\Delta^{-1}e^u\|^2 + \epsilon^2\|\nabla e^u\|^2 \le C(\|\nabla\Delta^{-1}e^u\| + \|\hat{\mathcal{R}}_1\|_{\mathring{H}^1(\Omega)'} + \|\hat{\mathcal{R}}_2\|_{\mathring{H}^1(\Omega)'})\|\nabla e^u\|.$$

Applying a Young inequality yields

$$\frac{\mathrm{d}}{\mathrm{d}t}\|\nabla\Delta^{-1}e^u\|^2 + \epsilon^2\|\nabla e^u\|^2 \le C\epsilon^{-2}\big(\|\nabla\Delta^{-1}e^u\|^2 + \|\hat{\mathcal{R}}_1\|^2_{\mathring{H}^1(\Omega)'} + \|\hat{\mathcal{R}}_2\|^2_{\mathring{H}^1(\Omega)'}\big),$$

and after use of a Gronwall inequality, results in

$$\sup_{t\in[0,T]}\|\nabla\Delta^{-1}e^u(t)\|^2 + \epsilon^2\int_0^T\|\nabla e^u\|^2\,\mathrm{d}t$$
$$\le C\,\mathrm{e}^{T/\epsilon^2}\left(\|\nabla\Delta^{-1}e^u(0)\|^2 + \epsilon^{-2}\int_0^T\left(\|\hat{\mathcal{R}}_1\|^2_{\mathring{H}^1(\Omega)'} + \|\hat{\mathcal{R}}_2\|^2_{\mathring{H}^1(\Omega)'}\right)\mathrm{d}t\right). \quad (23)$$

We then note from (21) and (20) that $\|\nabla\Delta^{-1}e^u(0)\| \le C_{\mathrm{P}}\|\hat{\mathcal{R}}_{\mathrm{IC}}\|$.

(II) Bound on e^μ. To bound e^μ in the $H^1(\Omega)'$-norm, we use the strategy of bounding two distincts part as in (16). First consider $\eta = 1$ in (14b):

$$(e^\mu, 1) = (\psi'(u) - \psi'(\hat{u}), 1) + \hat{\mathcal{R}}_2(1) \le L_{\psi'}\|e^u\||\Omega|^{1/2} + |\hat{\mathcal{R}}_2(1)|$$
$$\le C(\|\nabla e^u\| + \|\hat{\mathcal{R}}_2\|_{H^1(\Omega)'}).$$

Next consider $\eta \in \mathring{H}^1(\Omega)$:

$$\begin{aligned}(e^\mu, \eta) &= (\psi'(u) - \psi'(\hat{u}), \eta) + \epsilon^2(\nabla e^u, \nabla\eta) + \hat{\mathcal{R}}_2(\eta)\\ &\le L_{\psi'}\|e^u\|\|\eta\| + \epsilon^2\|\nabla e^u\|\|\nabla\eta\| + \|\hat{\mathcal{R}}_2\|_{\mathring{H}^1(\Omega)'}\|\nabla\eta\|\\ &\le \left(L_{\psi'}C_{\mathrm{P}}^2\|\nabla e^u\| + \epsilon^2\|\nabla e^u\| + \|\hat{\mathcal{R}}_2\|_{\mathring{H}^1(\Omega)'}\right)\|\nabla\eta\|\\ &\le C(\|\nabla e^u\| + \|\hat{\mathcal{R}}_2\|_{\mathring{H}^1(\Omega)'})\|\nabla\eta\|.\end{aligned}$$

Thus, substituting these two results in (16) (with $\hat{\mathcal{R}} = e^\mu$), we obtain

$$\|e^\mu\|_{H^1(\Omega)'} \le C(|(e^\mu, 1)| + \|e^\mu\|_{\mathring{H}^1(\Omega)'}) \le C(\|\nabla e^u\| + \|\hat{\mathcal{R}}_2\|_{H^1(\Omega)'}).$$

or

$$\epsilon^2\int_0^T \|e^\mu\|^2_{H^1(\Omega)'}\,\mathrm{d}t \le C\epsilon^2\int_0^T \left(\|\nabla e^u\|^2 + \|\hat{\mathcal{R}}_2\|^2_{H^1(\Omega)'}\right)\mathrm{d}t.$$

This shows that the error in μ is controlled by the error in u. Thus, upon substituting the bound on $\epsilon^2\int_0^T \|\nabla e^u\|^2\,\mathrm{d}t$ from (23), we finally have

$$\epsilon^2\int_0^T \|e^\mu\|^2_{H^1(\Omega)'}\,\mathrm{d}t \le C\,\mathrm{e}^{T/\epsilon^2}\left(\|\hat{\mathcal{R}}_{\mathrm{IC}}\|^2 + \epsilon^{-2}\int_0^T \left(\|\hat{\mathcal{R}}_1\|^2_{\mathring{H}^1(\Omega)'} + \|\hat{\mathcal{R}}_2\|^2_{H^1(\Omega)'}\right)\mathrm{d}t\right).$$

■

IV. GOAL-ORIENTED ERROR ANALYSIS

Given an arbitrary pair $(\hat{u}, \hat{\mu}) \in \mathcal{W} \times \mathcal{V}$ approximating the solution (u, μ) of (7), we shall be particularly interested in the error in certain quantities of interest. We assume that quantities of interest can be expressed as functionals $\mathcal{Q} : \mathcal{W} \times \mathcal{V} \to \mathbb{R}$ of the solution. For the sake of simplicity, we consider linear functionals of the form

$$\mathcal{Q}(u, \mu) = \bar{\mathcal{Q}}(u) + \tilde{\mathcal{Q}}(u, \mu) := (\bar{q}, u(T)) + \int_0^T (\langle q_1, u\rangle + (q_2, \mu))\,\mathrm{d}t, \tag{24}$$

where $\bar{q} \in H^1(\Omega)$, $q_1 \in L^2(0, T; H^1(\Omega)')$, and $q_2 \in L^2(0, T; H^1(\Omega))$.[5] The first part, $\bar{\mathcal{Q}}$, represents a quantity of interest totally defined on u at the final time T, and the other part, $\tilde{\mathcal{Q}}$, represents a space-time quantity of interest in u and μ. Because of linearity, we can write the error in $\mathcal{Q}$ as

$$\mathcal{Q}(u, \mu) - \mathcal{Q}(\hat{u}, \hat{\mu}) = \mathcal{Q}(e^u, e^\mu).$$

Remark 4.3. The ensuing analysis can be extended to continuously differentiable *nonlinear* functionals $\mathcal{Q}$ in the usual manner by linearization [41,44]. In particular, this extension is possible if the linearization yields a functional of the above form (24).

[5] The specified regularity on $\bar{q}$, q_1, and q_2 is such that we can establish well posedness of the dual Cahn–Hilliard problems; see Section V.

A. The Mean-Value-Linearized Backward-in-Time Dual

We first consider an exact error representation formula employing a mean-value-linearized dual problem. To write the dual problem in a concise form, we introduce an aggregated form of the weak formulation in (7). Let us define the following bilinear form $\mathcal{A}$, which collects all linear time-independent components, and the semilinear form $\mathcal{N}$, which represents the nonlinear term:

$$\mathcal{A}((u,\mu),(v,\eta)) := \int_0^T ((\nabla\mu,\nabla v) - \epsilon^2 (\nabla u,\nabla\eta) + (\mu,\eta))\, \mathrm{d}t, \tag{25a}$$

$$\mathcal{N}(u;\eta) := \int_0^T (\psi'(u),\eta)\, \mathrm{d}t. \tag{25b}$$

The weak formulation (7) can then be written as

$$\boxed{\begin{aligned}&\text{Find } (u,\mu) \in \mathcal{W}_{u_0} \times \mathcal{V} :\\ &\int_0^T \langle u_t, v\rangle\, \mathrm{d}t + \mathcal{A}\big((u,\mu),(v,\eta)\big) - \mathcal{N}(u;\eta) = 0 \qquad \forall (v,\eta) \in \mathcal{V}\times\mathcal{V}\,.\end{aligned}} \tag{26}$$

Note that the error equations (14a–14b) can be written concisely as

$$\int_0^T \langle e_t^u, v\rangle\, \mathrm{d}t + \mathcal{A}\big((e^u,e^\mu),(v,\eta)\big) - \mathcal{N}(u;\eta) + \mathcal{N}(\hat{u};\eta)$$
$$= \int_0^T (\hat{\mathcal{R}}_1(v) + \hat{\mathcal{R}}_2(\eta))\, \mathrm{d}t \qquad \forall (v,\eta) \in \mathcal{V}\times\mathcal{V}. \tag{27}$$

Following the generic goal-oriented error estimation framework in, for instance, [44, 47], we can obtain an exact representation formula for the error in $\mathcal{Q}$ by introducing the backward-in-time linearized-adjoint problem corresponding to our problem. The linearization has to be performed at a value in between u and $\hat{u}$. For this, let us introduce the so-called mean-value linearization of $\mathcal{N}$ (or secant form):

$$\mathcal{N}^{\mathrm{s}}(u,\hat{u};v,\eta) := \int_0^1 \mathcal{N}'(s\,u + (1-s)\hat{u};v,\eta)\, \mathrm{d}s,$$

where $\mathcal{N}'(w;v,\eta)$ is the Gâteaux (or Fréchet) derivative of $\mathcal{N}$ at w in the direction v, i.e.,

$$\mathcal{N}'(w;v,\eta) = \lim_{s\to 0} \frac{\mathcal{N}(w+sv;\eta) - \mathcal{N}(w;\eta)}{s}.$$

The main reason for introducing the mean-value-linearization is that, if the direction is chosen as the error, $v = e^u$, it is equal to the following difference:

$$\mathcal{N}^{\mathrm{s}}(u,\hat{u};e^u,\eta) = \mathcal{N}^{\mathrm{s}}(u,\hat{u};u-\hat{u},\eta) = \mathcal{N}(u;\eta) - \mathcal{N}(\hat{u};\eta). \tag{28}$$

To account for the "initial" condition for the backward-in-time problem, we denote

$$\mathcal{W}^{\bar{q}} := \{v \in \mathcal{W} \,:\, v(T) = \bar{q}\}.$$

We then define the following dual problem in terms of dual variables (p, χ):

$$\boxed{\begin{aligned}&\text{Find } (p,\chi) \in \mathcal{W}^{\bar{q}} \times \mathcal{V}:\\ &\quad -\int_0^T \langle p_t, v\rangle \, \mathrm{d}t + \mathcal{A}\big((v,\eta),(p,\chi)\big) - \mathcal{N}^{\mathrm{s}}(u,\hat{u};v,\chi) = \tilde{\mathcal{Q}}(v,\eta)\,,\\ &\qquad\qquad \forall (v,\eta) \in \mathcal{V}\times\mathcal{V}\,.\end{aligned}} \tag{29}$$

Note that the left-hand side corresponds to the mean-value linearized adjoint of the left-hand side of (26). We will analyze the well posedness and stability of this dual problem in Section V, see Corollary 5.1, where we show that there exists a unique dual solution which, moreover, satisfies

$$\|p\|^2_{L^\infty(0,T;H^1(\Omega))} + \epsilon^2\big(\|p_t\|^2_{\mathcal{V}'} + \|\chi\|^2_{\mathcal{V}}\big) \le C,$$

where C depends on Ω, $T\epsilon^{-2}$ and $\mathcal{Q}$.

It can be verified that the dual problem is a weak form of the following backward-in-time problem:

$$\left.\begin{aligned} -p_t + \epsilon^2\,\Delta\chi - \psi'^{\mathrm{s}}(u,\hat{u})\,\chi &= q_1\\ \chi - \Delta p &= q_2 \end{aligned}\right\} \quad \text{in } \Omega\times[0,T), \tag{30a}$$

$$\partial_n p = \partial_n \chi = 0 \qquad \text{on } \partial\Omega\times[0,T], \tag{30b}$$

$$p = \bar{q} \qquad \text{on } \Omega\times\{t=T\}, \tag{30c}$$

where the mean-value linearization of ψ' is defined analogously as

$$\psi'^{\mathrm{s}}(u,\hat{u}) = \int_0^1 \psi''(su + (1-s)\,\hat{u})\,\mathrm{d}s.$$

For the free energy function ψ given in (2), we can explicitly write $\psi'^{\mathrm{s}}(u,\hat{u})$ in terms of u and $\hat{u}$, although, because of its piecewise definition, this is an elaborate expression. For example, for $u,\hat{u} > 1$ or $u,\hat{u} < 1$, we have $\psi'^{\mathrm{s}}(u,\hat{u}) = 2$, and for $u,\hat{u} \in [-1,1]$, we have $\psi'^{\mathrm{s}}(u,\hat{u}) = u^2 + \hat{u}^2 + u\hat{u} - 1$. In particular, it should be noticed that if $\hat{u}$ and u are in the spinodal regime (where $\psi'' < 0$), i.e., $\hat{u}, u \in (-\frac{1}{3}\sqrt{3}, \frac{1}{3}\sqrt{3})$, then also $\psi'^{\mathrm{s}}(u,\hat{u}) < 0$. The fact that $\psi'^{\mathrm{s}}(u,\hat{u})$ can be negative is exactly what makes the stability analysis of (29) nontrivial (see Section V). In any case, since ψ' is Lipschitz continuous with $L_{\psi'} = 2$, see (3b), ψ'^{s} is at least bounded:

$$|\psi'^{\mathrm{s}}(u,\hat{u})| \le 2 \qquad \forall u,\hat{u} \in \mathbb{R}. \tag{31}$$

B. Error Representation

The dual problem (29) has been defined such that it provides an exact residual-based representation of the error in $\mathcal{Q}$.

Theorem 4.A (error representation). *Let* $(u, \mu) \in \mathcal{W}_{u_0} \times \mathcal{V}$ *denote the solution to* (7) *and* $(\hat{u}, \hat{\mu}) \in \mathcal{W} \times \mathcal{V}$ *denote any approximation. Let* $(p, \chi) \in \mathcal{W}^{\bar{q}} \times \mathcal{V}$ *denote the solution of the mean-value-linearized dual problem* (29). *Then the following error representation holds:*

$$\mathcal{Q}(u, \mu) - \mathcal{Q}(\hat{u}, \hat{\mu}) = \int_0^T (\hat{\mathcal{R}}_1(p) + \hat{\mathcal{R}}_2(\chi))\,\mathrm{d}t + \hat{\mathcal{R}}_{\mathrm{IC}}(p(0)). \tag{32}$$

Proof. We proceed by following the general scheme of invoking the dual problem, integration by parts, a linearization formula and, finally, the primal problem in the form of the error equation. Hence, noting that $e^u \in \mathcal{W} \subset \mathcal{V}$ and $e^\mu \in \mathcal{V}$, we obtain from the dual (29) that

$$\begin{aligned}\mathcal{Q}(u, \mu) - \mathcal{Q}(\hat{u}, \hat{\mu}) &= \tilde{\mathcal{Q}}(e^u, e^\mu) + \bar{\mathcal{Q}}(e^u) \\ &= -\int_0^T \langle p_t, e^u \rangle\,\mathrm{d}t + \mathcal{A}((e^u, e^\mu), (p, \chi)) - \mathcal{N}^{\mathrm{s}}(u, \hat{u}; e^u, \chi) + (\bar{q}, e^u(T)).\end{aligned}$$

Integrating by parts in time, see (6), and using $p(T) = \bar{q}$,

$$\mathcal{Q}(u, \mu) - \mathcal{Q}(\hat{u}, \hat{\mu}) = \int_0^T \langle e^u_t, p \rangle\,\mathrm{d}t + \mathcal{A}((e^u, e^\mu), (p, \chi)) - \mathcal{N}^{\mathrm{s}}(u, \hat{u}; e^u, \chi) + (p(0), e^u(0)).$$

Next, we invoke the mean-value linearization property (28), and $e^u(0) = u_0 - \hat{u}(0)$,

$$\begin{aligned}&\mathcal{Q}(u, \mu) - \mathcal{Q}(\hat{u}, \hat{\mu}) \\ &\quad = \int_0^T \left\langle e^u_t, p \right\rangle \mathrm{d}t + \mathcal{A}((e^u, e^\mu), (p, \chi)) - \mathcal{N}(u; \chi) + \mathcal{N}(\hat{u}; \chi) + (p(0), u_0 - \hat{u}(0)).\end{aligned}$$

The proof then follows by subtituting the error equation (27) with $(v, \eta) = (p, \chi)$ (since $p \in \mathcal{W}^{\bar{q}} \subset \mathcal{V}$ and $\chi \in \mathcal{V}$) and by definition of the initial condition residual (12c). ∎

Theorem 4.A holds for arbitrary approximations $(\hat{u}, \hat{\mu}) \in \mathcal{W} \times \mathcal{V}$, in particular for the semi-discrete approximation (u^h, μ^h) described in Section II C. However, for Galerkin-based approximations, such as (u^h, μ^h), we have a stronger result, since residuals vanish for discrete test functions. Moreover, we can invoke Proposition 3.1 to obtain an abstract a priori bound. We summarize this in the following.

Corollary 4.2. *Under the assumptions of Theorem 4.A, with the exception that* $(\hat{u}, \hat{\mu}) = (u^h, \mu^h)$ *denotes the semi-discrete solution to* (9)*, the following error representation holds:*

$$\begin{aligned}\mathcal{Q}(u, \mu) - \mathcal{Q}(u^h, \mu^h) = \int_0^T (\mathcal{R}_1((u^h, \mu^h); p - v^h) + \mathcal{R}_2((u^h, \mu^h); \chi - \eta^h))\,\mathrm{d}t \\ + \mathcal{R}_{\mathrm{IC}}(u^h(0); p(0) - w^h).\end{aligned} \tag{33}$$

for any $v^h \in L^2(0,T;S^h)$, $\eta^h \in L^2(0,T;S^h)$, and $w^h \in S^h$. Moreover, the following a priori estimate holds:

$$|\mathcal{Q}(u,\mu) - \mathcal{Q}(u^h,\mu^h)| \leq C\left(\|e^u(0)\|^2 + \int_0^T \left(\|e_t^u\|^2_{\mathring{H}^1(\Omega)'} + \|e^u\|^2_{\mathring{H}^1(\Omega)} + \|e^\mu\|^2_{H^1(\Omega)}\right)\mathrm{d}t\right)^{1/2}$$
$$\times\left(\inf_{v^h\in L^2(0,T;S^h)}\int_0^T \|\nabla(p - v^h)\|^2\,\mathrm{d}t\right.$$
$$\left.+ \inf_{\eta^h\in L^2(0,T;S^h)}\int_0^T \|\chi - \eta^h\|^2_{H^1(\Omega)}\,\mathrm{d}t + \inf_{w^h\in S^h}\|p(0) - w^h\|\right)^{1/2},$$

where C is the constant in Proposition 3.1.

Remark 4.3. Note that the a priori estimate is a product of two error contributions (primal and dual) signifying the higher-order convergence in quantities of interest that can be expected for Galerkin-based approximations [68].

Proof (of Corollary 4.2). The error representation formula simply follows from Theorem 4.A applied to (u^h,μ^h), together with the observation that the residuals $\mathcal{R}_1$, $\mathcal{R}_2$, and $\mathcal{R}_{\mathrm{IC}}$ vanish for discrete test functions owing to (9a), (9b), and (9c), respectively. To prove the a priori estimate, we first apply Cauchy–Schwartz inequalities to (33):

$$|\mathcal{Q}(u,\mu) - \mathcal{Q}(u^h,\mu^h)| \leq \left(\int_0^T \|\mathcal{R}_1((u^h,\mu^h);\cdot)\|^2_{\mathring{H}^1(\Omega)'}\,\mathrm{d}t\right)^{1/2}\left(\int_0^T \|\nabla(p - v^h)\|^2\,\mathrm{d}t\right)^{1/2}$$
$$+\left(\int_0^T \|\mathcal{R}_2((u^h,\mu^h);\cdot)\|^2_{H^1(\Omega)'}\,\mathrm{d}t\right)^{1/2}\left(\int_0^T \|\chi - \eta^h\|^2_{H^1(\Omega)}\,\mathrm{d}t\right)^{1/2}$$
$$+\|\mathcal{R}_{\mathrm{IC}}(u^h(0);\cdot)\|\,\|p(0) - w^h\|.$$

Notice that to bound $\mathcal{R}_1$, we could use $\mathcal{R}_1((u^h,\mu^h);1) = 0$ as u^h satisfies mass conservation (10). The a priori estimate then follows by applying a discrete Hölder inequality to the right-hand side, invoking Proposition 3.1, and taking the inf with respect to the discrete test functions. ∎

C. Computable Error Estimate

To obtain a computable estimate of the error, we shall employ approximations to the dual problem. In particular, notice that the mean-value-linearized dual problem (29) depends on the unknown solution u. A straightforward approximation involves replacing u in (29) by the approximation $\hat{u} \in \mathcal{W}$, which essentially corresponds to replacing the mean-value linearization by the linearization at $\hat{u}$. We thus have the dual problem:

$$\begin{aligned}&\text{Find } (p,\chi) \in \mathcal{W}^{\bar{q}} \times \mathcal{V}:\\ &\quad -\int_0^T \langle p_t, v\rangle\,\mathrm{d}t + \mathcal{A}\big((v,\eta),(p,\chi)\big) - \mathcal{N}'(\hat{u};v,\chi) = \tilde{\mathcal{Q}}(v,\eta),\\ &\qquad \forall (v,\eta) \in \mathcal{V}\times\mathcal{V}.\end{aligned} \tag{34}$$

The well posedness and stability of this dual problem is analogous to the mean-value-linearized dual problem and it will also be established in Section V, see Corollary 5.1.

Dual problem (34) is a weak form of the following backward-in-time problem:

$$\left.\begin{aligned} -p_t + \epsilon^2 \Delta\chi - \psi''(\hat{u})\,\chi &= q_1 \\ \chi - \Delta p &= q_2 \end{aligned}\right\} \quad \text{in } \Omega \times [0,T), \tag{35a}$$

$$\partial_n p = \partial_n \chi = 0 \qquad \text{on } \partial\Omega \times [0,T], \tag{35b}$$

$$p = \bar{q} \qquad \text{on } \Omega \times \{t = T\}, \tag{35c}$$

where for ψ given in (2) we have

$$\psi''(\hat{u}) = \begin{cases} 2 & \hat{u} \notin [-1,1], \\ 3\hat{u}^2 - 1 & \hat{u} \in [-1,1]. \end{cases} \tag{36}$$

Instead of an exact residual-based representation of the error in $\mathcal{Q}$, we now pick up a remainder term.

Theorem 4.B (error representation with remainder). *Let $(u,\mu) \in \mathcal{W}_{u_0} \times \mathcal{V}$ denote the solution to* (7) *and $(\hat{u},\hat{\mu}) \in \mathcal{W} \times \mathcal{V}$ denote any approximation. Let $(p,\chi) \in \mathcal{W}^{\bar{q}} \times \mathcal{V}$ denote the solution of the linearized dual problem* (34)*. Then the following error representation holds:*

$$\mathcal{Q}(u,\mu) - \mathcal{Q}(\hat{u},\hat{\mu}) = \int_0^T (\hat{\mathcal{R}}_1(p) + \hat{\mathcal{R}}_2(\chi))\,\mathrm{d}t + \hat{\mathcal{R}}_{\mathrm{IC}}(p(0)) + r, \tag{37}$$

with higher-order remainder

$$r := \int_0^T \int_\Omega \int_0^1 (1-s)\psi'''(su + (1-s)\hat{u})\,\mathrm{d}s\,(e^u)^2\,\chi\,\mathrm{d}x\,\mathrm{d}t. \tag{38}$$

For $\hat{u} \in \hat{W} \subset L^\infty(0,T;H^1(\Omega))$, r can be bounded as follows:

$$|r| \le 3\|e^u\|^2_{L^4(0,T;L^4(\Omega))}\|\chi\|_{L^2(0,T;L^2(\Omega))}.$$

Remark 4.4. To see that the bound on the remainder r makes sense, first note that $\chi \in \mathcal{V} \subset L^2(0,T;L^2(\Omega))$ and $u,\hat{u} \in L^\infty(0,T;H^1(\Omega))$ (see (8)). Then, $e^u \in L^4(0,T;L^4(\Omega))$ (in $\mathbb{R}^d$, $d = 1,\ldots,4$) by a Sobolov inequality.

Proof (of Theorem 4.B). To obtain the error representation formula, we proceed similarly as in the proof of Theorem 4.A: invoking the dual problem, integration by parts, a Taylor series formula and, finally, the primal problem in the form of the error equation. Thus, using dual (34) and subsequently integrating by parts in time (6), using $p(T) = \bar{q}$, we obtain

$$\begin{aligned} \mathcal{Q}(u,\mu) - \mathcal{Q}(\hat{u},\hat{\mu}) &= \tilde{\mathcal{Q}}(e^u,e^\mu) + \bar{\mathcal{Q}}(e^u) \\ &= -\int_0^T \langle p_t, e^u\rangle\,\mathrm{d}t + \mathcal{A}((e^u,e^\mu),(p,\chi)) - \mathcal{N}'(\hat{u};e^u,\chi) + (\bar{q},e^u(T)) \\ &= \int_0^T \langle e^u_t, p\rangle\,\mathrm{d}t + \mathcal{A}((e^u,e^\mu),(p,\chi)) - \mathcal{N}'(\hat{u};e^u,\chi) + (p(0),e^u(0)) \end{aligned} \tag{39}$$

Recall the following Taylor series formula with exact remainder,

$$\mathcal{N}(u;\chi) = \mathcal{N}(\hat{u};\chi) + \mathcal{N}'(\hat{u};e^u,\chi) + r_{\mathcal{N}},$$

where

$$r_{\mathcal{N}} = \int_0^1 (1-s)\mathcal{N}''(su + (1-s)\hat{u}; e^u, e^u, \chi)\,\mathrm{d}s,$$

and the second derivative is defined recursively as

$$\mathcal{N}''(\tilde{u};v,w,\eta) = \lim_{s\to 0} \frac{\mathcal{N}'(\tilde{u}+sw;v,\eta) - \mathcal{N}'(\tilde{u};v,\eta)}{s}.$$

Using the definition of $\mathcal{N}$ in (25b), we can establish that $r_{\mathcal{N}}$ is equal to the remainder r in (38). Substituting the Taylor series formula in (39), we obtain

$$\begin{aligned}\mathcal{Q}(u,\mu) &- \mathcal{Q}(\hat{u},\hat{\mu})\\ &= \int_0^T \langle e_t^u, p\rangle\,\mathrm{d}t + \mathcal{A}((e^u,e^\mu),(p,\chi)) - \mathcal{N}(u;\chi) + \mathcal{N}(\hat{u};\chi) + r + (p(0),e^u(0))\end{aligned}$$

The error representation then follows by subtituting the error equation (27) and by definition of the initial condition residual (12c). To prove the bound on the remainder r, we use that $|\psi'''(u)| \le 6$ for all $u \in \mathbb{R}$, yielding

$$|r| \le 3\int_0^T \int_\Omega (e^u)^2|\chi|\,\mathrm{d}x\,\mathrm{d}t.$$

The bound then follows from a generalized Hölder inequality. ∎

In practice, to obtain a computable estimate, one discretizes the dual problem yielding dual approximations $(\hat{p},\hat{\chi}) \in \mathcal{W}\times\mathcal{V}$. A coarse estimate of the error in $\mathcal{Q}$ can then be computed by neglecting the error in the dual solution $(e^p,e^\chi) = (p-\hat{p},\chi-\hat{\chi})$ as well as the linearization error captured by r:

$$\mathcal{Q}(u,\mu) - \mathcal{Q}(\hat{u},\hat{\mu}) \approx \mathrm{Est}(\hat{u},\hat{\mu};\hat{p},\hat{\chi}) := \int_0^T (\hat{\mathcal{R}}_1(\hat{p}) + \hat{\mathcal{R}}_2(\hat{\chi}))\,\mathrm{d}t + \hat{\mathcal{R}}_{\mathrm{IC}}(\hat{p}(0)). \tag{40}$$

Of course, this estimate can only be accurate if the neglected terms are sufficiently small. For example, if $(\hat{p},\hat{\chi})$ is computed with a higher-order method (or with a finer mesh) than for $(\hat{u},\hat{\mu})$, and the exact solutions (u,μ) and (p,χ) are sufficiently smooth, then the neglected terms are of higher-order. A true upper bound on the error in $\mathcal{Q}$ would involve controlling the error (e^p,e^χ) as well as the remainder r.

V. ANALYSIS OF DUAL CAHN–HILLIARD PROBLEMS

Duals of nonlinear problems have mostly been analyzed in the context of error estimation for weaker norms (Aubin-Nitsche trick) or quantities of interest. Examples of time-independent nonlinear problems include quasi-linear elliptic problems [69] and free-boundary problems [70, 71].

Examples of time-dependent nonlinear problems include nonlinear conservation laws [72] and nonlinear parabolic problems [58, 73].

In this section, we shall analyze the following dual Cahn–Hilliard problem, written as a forward problem after the change of variable $t \mapsto T - t$:

$$\begin{aligned}
&\text{Find } (p,\chi) \in \mathcal{W}_{\bar q} \times \mathcal{V}: \\
&\langle p_t(t), v\rangle - \big(\phi(t)\,\chi(t), v\big) - \epsilon^2\big(\nabla\chi(t), \nabla v\big) = \big(q_1(t), v\big) \qquad \forall v \in H^1(\Omega), \qquad (41a)\\
&\big(\chi(t), \eta\big) + \big(\nabla p(t), \nabla\eta\big) = \big(q_2(t), \eta\big) \qquad \forall \eta \in H^1(\Omega), \qquad (41b)\\
&\qquad \text{a.e. } 0 \le t \le T,
\end{aligned}$$

where $\phi \in L^\infty(0,T; L^\infty(\Omega))$ is a given coefficient satisfying for some $C_\phi > 0$,

$$-C_\phi \le \phi(t,x) \le C_\phi, \quad \text{a.e. } (t,x) \in [0,T] \times \Omega.$$

The difficulty is that ϕ can be smaller than 0. The main result of this section is the following.

Theorem 5.A (dual well posedness). *The dual Cahn–Hilliard problem* (41) *has a unique weak solution* $(p,\chi) \in \mathcal{W}_{\bar q} \times \mathcal{V}$. *Moreover, the solution satisfies the a priori estimate*

$$\begin{aligned}
&(1 + T/\epsilon^2)^{-1} \sup_{t\in[0,T]} \|p(t)\|^2_{H^1(\Omega)} + \epsilon^2\big(\|p_t\|^2_{\mathcal{V}'} + \|\chi\|^2_{\mathcal{V}}\big) \\
&\quad \le C\, \mathrm{e}^{T/\epsilon^2} \big(\|\bar q\|^2_{H^1(\Omega)} + \epsilon^{-2}\|q_1\|^2_{\mathcal{V}'} + \|q_2\|^2_{\mathcal{V}}\big). \qquad (42)
\end{aligned}$$

Before we go into the proof of this theorem, we first observe that since the dual (41) is closely related to the dual problems introduced in the previous section, we immediately have the following.

Corollary 5.1. *The mean-value-linearized dual problem* (29) *and the linearized dual problem* (34) *have unique solutions* $(p,\chi) \in \mathcal{W}^{\bar q} \times \mathcal{V}$ *which, moreover, satisfy the estimate* (42).

Proof. By a change of variable $t \mapsto T - t$, problems (29) and (34) change into the form of (41) with $\phi = \psi'^{\mathrm{s}}(u,\hat u)$ and $\phi = \psi''(\hat u)$, respectively. Furthermore, in both cases $|\phi| \le 2$, see (31) and (36). The result then follows from Theorem 5.A. ∎

To establish the existence of a solution to (41), we use the Faedo–Galerkin technique; see, e.g., [64, 65, 74, 75]. That is, we consider a sequence of approximations (p^m, χ^m), $m = 0, 1, 2, \ldots$, for which we show a priori bounds, implying a weakly convergent subsequence, the limit of which satisfies the weak formulation (41).

A. Faedo–Galerkin Approximations

Let $\{w_k\}_{k=0}^\infty$ denote the $H^1(\Omega)$-orthogonal and $L^2(\Omega)$-orthonormal basis given by the eigenfunctions of the Laplace operator: $-\Delta w_k = \lambda_k\, w_k$ in Ω, with boundary conditions $\partial_n w_k = 0$ on $\partial\Omega$ (ordered as $0 = \lambda_0 \le \lambda_1 \le \cdots$). Consider the following semi-discrete approximation with respect to $S^m := \mathrm{span}\{w_0, \ldots, w_m\} \subset H^1(\Omega)$:

$$p^m(t) := \sum_{k=0}^m c_k^m(t)\, w_k, \qquad \chi^m(t) := \sum_{k=0}^m d_k^m(t)\, w_k,$$

such that for a.e. $0 < t \leq T$:

$$(\partial_t p^m(t), v) - (\phi(t)\,\chi^m(t), v) - \epsilon^2(\nabla\chi^m(t), \nabla v) = (q_1(t), v) \quad \forall v \in S^m, \tag{43a}$$

$$(\chi^m(t), \eta) + (\nabla p^m(t), \nabla\eta) = (q_2(t), \eta) \quad \forall \eta \in S^m, \tag{43b}$$

$$(p^m(0) - \bar{q}, \xi) = 0 \qquad \forall \xi \in S^m. \tag{43c}$$

This reduces to the following initial value problem for the coefficients $(c^m, d^m) = ((c_0^m, \ldots, c_m^m), (d_0^m, \ldots, d_m^m))$:

$$\frac{\mathrm{d}}{\mathrm{d}t}c_k^m - D_k(t)d^m - \epsilon^2\lambda_k d_k^m = q_{1,k} \quad \forall k = 0, \ldots, m, \tag{44a}$$

$$d_k^m + \lambda_k c_k^m = q_{2,k} \quad \forall k = 0, \ldots, m, \tag{44b}$$

$$c_k^m(0) = \bar{q}_k \qquad \forall k = 0, \ldots, m. \tag{44c}$$

where $q_{1,k} := (q_1, w_k)$, $q_{2,k} := (q_2, w_k)$, $\bar{q}_k := (\bar{q}, w_k)$, and

$$D_k(t)d^m := \sum_{j=1}^{m}(\phi(t)w_j, w_k)\, d_j^m.$$

Eliminating d^m from (44a) using (44b), we obtain

$$\frac{\mathrm{d}}{\mathrm{d}t}c_k^m + \lambda_k C_k(t)c^m = q_{1,k} + C_k(t)q_{2,k} \qquad \forall k, \tag{44a$'$}$$

where $C_k(t)(\cdot) := \epsilon^2\lambda_k(\cdot)_k + D_k(t)(\cdot)$. Eqs. (44a′) and (44c) now form a system of linear ordinary differential equations for c^m, which has a unique absolute continuous solution owing to standard existence theory. Accordingly, since d^m is defined via (44b), there is a unique pair $(p^m, \chi^m) \in C([0,T]; S^m) \times L^2(0,T; S^m)$ with $\partial_t p^m \in L^2(0,T; S^m)$ which satisfies (43).

B. A Priori Estimates

Before presenting the a priori estimates for the dual (43), let us briefly discuss the main idea behind obtaining these. Contrary to the nonlinear Cahn–Hilliard equation, there is no Lyapunov energy functional for its dual (43). However, analogous to the Cahn–Hilliard equation, one can still obtain a fundamental energy estimate for (43) by substituting $v = -\chi^m$ and $\eta = \partial_t p^m$ in (43a) and (43b), respectively, and adding both equations. In that case, noting that the $(\partial_t p^m, \chi^m)$ terms cancel, we get

$$\frac{1}{2}\frac{\mathrm{d}}{\mathrm{d}t}\|\nabla p^m\|^2 + \epsilon^2\|\nabla\chi^m\|^2 = -\int_\Omega \phi|\chi^m|^2\,\mathrm{d}x \leq C_\phi\|\chi^m\|^2, \tag{45}$$

where for the sake of the argument, we have left out the q_1 and q_2-terms.[6] Since we only have minor (ϵ^2) control of $\|\nabla\chi^m\|^2$ on the left-hand side, the key element now is to bound $\|\chi^m\|^2$ on the

[6]Note that in the case of $0 \leq \phi \leq C_\phi$, the right-hand side of (45) vanishes, and, after integrating with respect to time, we would obtain a stability estimate implying no growth. However, in general, ϕ can be negative which reflects the exponential growth behavior of the Cahn–Hilliard equation in the spinodal regime.

right-hand side in terms of both $\|\nabla\chi^m\|$ and $\|\nabla p^m\|$. Such a Poincaré-type inequality is readily obtained by substituting $\eta = \chi^m$ in (43b) (omitting q_2):

$$\|\chi^m\|^2 = -(\nabla p^m, \nabla\chi^m) \le \|\nabla p^m\|\|\nabla\chi^m\| \le \frac{C_\phi}{2\epsilon^2}\|\nabla p^m\|^2 + \frac{\epsilon^2}{2C_\phi}\|\nabla\chi^m\|^2.$$

Inserting this result in (45) and invoking a Gronwall inequality results in the desired a priori bound. Of course, if q_1 and q_2 are present, these have to be taken care of appropriately. We summarize the general result in the following.

Lemma 5.2. *There is a constant C, depending on Ω, but independent of m, T, and ϵ, such that*

$$\|p^m(0)\|_{H^1(\Omega)} \le \|\bar{q}\|_{H^1(\Omega)},$$

$$\sup_{t\in[0,T]} \|\nabla p^m(t)\|^2 + \epsilon^2\int_0^T \|\nabla\chi^m\|^2\,\mathrm{d}t \le C\,\mathrm{e}^{T/\epsilon^2}\left(\|\bar{q}\|^2_{H^1(\Omega)} + \epsilon^{-2}\|q_1\|^2_{\mathcal{V}'} + \|q_2\|^2_{\mathcal{V}}\right).$$

Proof. We split the proof in 4 steps.

(I) Fundamental estimates. Take $v = -\chi^m$ and $\eta = \partial_t p^m$ in (43a) and (43b), respectively, add both equations and use Cauchy–Schwarz inequalities:

$$\boxed{\begin{aligned}&\frac{1}{2}\frac{\mathrm{d}}{\mathrm{d}t}\|\nabla p^m\|^2 + \epsilon^2\|\nabla\chi^m\|^2\\ &\qquad \le C_\phi\|\chi^m\|^2 + \|q_1\|_{H^1(\Omega)'}\|\chi^m\|_{H^1(\Omega)} + \|q_2\|_{H^1(\Omega)}\|\partial_t p^m\|_{H^1(\Omega)'}\,.\end{aligned}} \tag{46a}$$

As explained above, we shall bound $\|\chi^m\|^2$ using the estimate obtained by setting $\eta = \chi^m$ in (43b):

$$\|\chi^m\|^2 \le \|\nabla p^m\|\|\nabla\chi^m\| + \|q_2\|\|\chi^m\|,$$

or, after applying a Young inequality, we get

$$\boxed{\|\chi^m\|^2 \le 2\|\nabla p^m\|\|\nabla\chi^m\| + \|q_2\|^2\,.} \tag{46b}$$

Note that the q_2-term in (46a) forces us to estimate $\partial_t p^m$ before we can continue.

(II) Estimate of $\partial_t p^m$ in terms of χ^m. Consider $v = v^m + v^\perp \in H^1(\Omega)$ with $v^m \in S^m$ and $(v^\perp, w_k) = 0$ for all $k = 0, \ldots, m$. Owing to our choice of $\{w_k\}$, this implies $(\nabla v^\perp, \nabla w_k) = 0$ as well. Thus, $\|v^m\|^2_{H^1(\Omega)} = \|v\|^2_{H^1(\Omega)} - \|v^\perp\|^2_{H^1(\Omega)} \le \|v\|^2_{H^1(\Omega)}$. Next, noting that $(\partial_t p^m, v) = (\partial_t p^m, v^m)$, we obtain from (43a):

$$\begin{aligned}(\partial_t p^m, v) &= \langle q_1, v^m\rangle + (\phi\,\chi^m, v^m) + \epsilon^2(\nabla\chi^m, \nabla v^m)\\ &\le \|q_1\|_{H^1(\Omega)'}\|v^m\|_{H^1(\Omega)} + C_\phi\|\chi^m\|\|v^m\| + \epsilon^2\|\nabla\chi^m\|\|\nabla v^m\|\\ &\le (\|q_1\|_{H^1(\Omega)'} + C_\phi\|\chi^m\| + \epsilon^2\|\nabla\chi^m\|)\|v\|_{H^1(\Omega)}.\end{aligned}$$

So

$$\boxed{\|\partial_t p^m\|_{H^1(\Omega)'} \le \|q_1\|_{H^1(\Omega)'} + C_\phi\|\chi^m\| + \epsilon^2\|\nabla\chi^m\|\,.} \tag{47}$$

(III) Bound on initial condition. At this moment, we pick up along the way the bound on $p^m(0)$. Indeed, decomposing $\bar{q} \in H^1(\Omega)$ into $\bar{q}^m \in S^m$ and $\bar{q}^\perp$ as in step (II), it easily follows from (43c) that:

$$\boxed{\|p^m(0)\|_{H^1(\Omega)} \leq \|\bar{q}\|_{H^1(\Omega)}\,.} \tag{48}$$

(IV) Bound on gradients. Substituting (47) into the fundamental estimate (46a), we obtain

$$\begin{aligned}\frac{1}{2}\frac{\mathrm{d}}{\mathrm{d}t}\|\nabla p^m\|^2 + \epsilon^2\|\nabla\chi^m\|^2 &\leq C_\phi\|\chi^m\|^2 + \|q_1\|_{H^1(\Omega)'}(\|\chi^m\| + \|\nabla\chi^m\|)\\ &\quad + \|q_2\|_{H^1(\Omega)}(\|q_1\|_{H^1(\Omega)'} + C_\phi\|\chi^m\| + \epsilon^2\|\nabla\chi^m\|)\\ &\leq \left(\frac{3}{2}C_\phi + \frac{1}{2}\right)\|\chi^m\|^2 + \frac{\epsilon^2}{4}\|\nabla\chi^m\|^2\\ &\quad + (1+2\epsilon^{-2})\|q_1\|^2_{H^1(\Omega)'} + \left(\frac{1}{2}C_\phi + \frac{1}{2} + 2\epsilon^2\right)\|q_2\|^2_{H^1(\Omega)},\end{aligned}$$

where we employed various Young inequalities in the last step, in particular to obtain $\frac{\epsilon^2}{4}\|\nabla\chi^m\|^2$ on the right-hand side. Next, we substitute the estimate for $\|\chi^m\|^2$, see (46b),

$$\begin{aligned}\frac{1}{2}\frac{\mathrm{d}}{\mathrm{d}t}\|\nabla p^m\|^2 + \epsilon^2\|\nabla\chi^m\|^2 &\leq \left(\frac{3}{2}C_\phi + \frac{1}{2}\right)(2\|\nabla p^m\|\|\nabla\chi^m\| + \|q_2\|^2) + \frac{\epsilon^2}{4}\|\nabla\chi^m\|^2\\ &\quad + (1+2\epsilon^{-2})\|q_1\|^2_{H^1(\Omega)'} + \left(\frac{1}{2}C_\phi + \frac{1}{2} + 2\epsilon^2\right)\|q_2\|^2_{H^1(\Omega)}\\ &\leq 2\epsilon^{-2}(3C_\phi + 1)^2\|\nabla p^m\|^2 + \frac{\epsilon^2}{2}\|\nabla\chi^m\|^2\\ &\quad + C\big(\epsilon^{-2}\|q_1\|^2_{H^1(\Omega)'} + \|q_2\|^2_{H^1(\Omega)}\big),\end{aligned}$$

where we picked up another $\frac{\epsilon^2}{4}\|\nabla\chi^m\|^2$ in the last step. So, we finally arrive at

$$\boxed{\frac{\mathrm{d}}{\mathrm{d}t}\|\nabla p^m\|^2 + \epsilon^2\|\nabla\chi^m\|^2 \leq C\left(\epsilon^{-2}\|\nabla p^m\|^2 + \epsilon^{-2}\|q_1\|^2_{H^1(\Omega)'} + \|q_2\|^2_{H^1(\Omega)}\right)\,.}$$

Invoking a Gronwall inequality and the bound (48) on the initial condition proves the Lemma. ■

Lemma 5.2 took care of the gradients. To have full control in $H^1(\Omega)$, we next consider a bound on the averages.

Lemma 5.3. *There is a constant C, depending on Ω, but independent of m, T, and ϵ, such that*

$$\left(\int_\Omega \chi^m(t)\,\mathrm{d}x\right)^2 = \left(\int_\Omega q_2(t)\,\mathrm{d}x\right)^2 \qquad \textit{a.e. } t \in [0,T],$$

$$\sup_{t\in[0,T]}\left(\int_\Omega (p^m(t) - \bar{q})\,\mathrm{d}x\right)^2 \leq C\frac{T}{\epsilon^2}\,\mathrm{e}^{T/\epsilon^2}\,\big(\|\bar{q}\|^2_{H^1(\Omega)} + \epsilon^{-2}\|q_1\|^2_{\mathcal{V}'} + \|q_2\|^2_{\mathcal{V}}\big).$$

Proof. The average of χ^m follows easily from (43b) by taking $\eta = 1$. In particular, we then obtain a bound on $\|\chi^m\|$ by a Poincaré–Friedrichs inequality:

$$\epsilon^2 \int_0^T \|\chi^m\|^2 \,\mathrm{d}t \le C\epsilon^2 \int_0^T \left(\left(\int_\Omega \chi^m(t)\,\mathrm{d}x \right)^2 + \|\nabla \chi^m\|^2 \right) \mathrm{d}t$$
$$\le C\,\mathrm{e}^{T/\epsilon^2} \left(\|\bar{q}\|^2_{H^1(\Omega)} + \epsilon^{-2}\|q_1\|^2_{\mathcal{V}'} + \|q_2\|^2_{\mathcal{V}} \right), \tag{49}$$

where we used Lemma 5.2 in the last step. Next, consider (43a) with $v = 1$ and integrate with respect to t:

$$\int_\Omega (p^m(t) - p^m(0))\,\mathrm{d}x = \int_0^t \langle q_1, 1\rangle \,\mathrm{d}t + \int_0^t \int_\Omega \phi\,\chi^m \,\mathrm{d}x\,\mathrm{d}t$$
$$\le \int_0^t \|q_1\|_{H^1(\Omega)'}\,\mathrm{d}t + C_\phi \int_0^t \int_\Omega |\chi^m|\,\mathrm{d}x\,\mathrm{d}t$$
$$\le t \left(\int_0^t \|q_1\|^2_{H^1(\Omega)'}\,\mathrm{d}t \right)^{1/2} + C_\phi |\Omega| t \left(\int_0^t \|\chi^m\|^2\,\mathrm{d}t \right)^{1/2}$$

The proof then follows by noting that $\int_\Omega p^m(0)\,\mathrm{d}x = \int_\Omega \bar{q}\,\mathrm{d}x$ and inserting the just derived bound on $\|\chi^m\|$ in (49). ■

Notice that Lemma (5.3) shows that the average of χ^m follows perfectly the average of q_2, whereas the average of p^m generally diverges from its initial average as fast as $O(T\epsilon^{-2}\exp(T\epsilon^{-2}))$.

A bound on the time-derivative $\partial_t p^m$ can furthermore be established, now that we have obtained a bound on $\|\chi^m\|$.

Corollary 5.4. *There is a constant C, depending on Ω, but independent of m, T, and ϵ, such that*

$$\epsilon^2 \|\partial_t p^m\|^2_{\mathcal{V}'} \le C\,\mathrm{e}^{T/\epsilon^2} \left(\|\bar{q}\|^2_{H^1(\Omega)} + \epsilon^{-2}\|q_1\|^2_{\mathcal{V}} + \|q_2\|^2_{\mathcal{V}'} \right).$$

Proof. Going back to (47), we can estimate the right-hand side with available bounds:

$$\int_0^T \|\partial_t p^m\|^2_{H^1(\Omega)'}\,\mathrm{d}t \le C \int_0^T \left(\|q_1\|^2_{H^1(\Omega)'} + \|\chi^m\|^2 + \epsilon^4 \|\nabla\chi^m\|^2 \right) \mathrm{d}t$$
$$\le C\epsilon^{-2}\,\mathrm{e}^{T/\epsilon^2} \left(\|\bar{q}\|^2_{H^1(\Omega)} + \epsilon^{-2}\|q_1\|^2_{\mathcal{V}'} + \|q_2\|^2_{\mathcal{V}} \right),$$

where we substituted the bound (49) on $\|\chi^m\|$. ■

C. Proof of Theorem 5.A

To finish the proof of existence, we resort to the classical weak compactness argument: The above-derived a priori estimates imply the existence of a subsequence $\{(p^{m_l}, \chi^{m_l})\}_{l=1}^\infty$ that converges weakly to a pair $(p, \chi) \in \mathcal{W} \times \mathcal{V}$, i.e.,

$$\left.\begin{array}{lll} p^{m_l} & \rightharpoonup p & \text{weakly in } L^\infty(0,T;H^1(\Omega)) \subset \mathcal{W} \\ \partial_t p^{m_l} & \rightharpoonup \partial_t p & \text{weakly in } \mathcal{V}' \\ \chi^{m_l} & \rightharpoonup \chi & \text{weakly in } \mathcal{V} \end{array}\right\} \quad \text{as } l \to \infty.$$

It can be shown, by passing to the limit in (43) in the usual manner, that the pair (p, χ) satisfies the weak formulation (41). This completes the proof of existence. Since the a priori estimates are independent of m_l, they hold for (p, χ) as well. The total estimate (42) is obtained by combining the estimates in Lemmas 5.2 and 5.3, (49), and Corollary 5.4.

To establish uniqueness, let (p_1, χ_1) and (p_2, χ_2) denote two solutions to (41). Their difference $(d^p, d^\chi) := (p_1 - p_2, \chi_1 - \chi_2)$ satisfies (41) with $\bar{q} = q_1 = q_2 = 0$. Taking $v = d^p(t)$ and $\eta = \epsilon^2 d^\chi(t)$ in (41a) and (41b), respectively, and adding both equations gives

$$\frac{1}{2}\frac{\mathrm{d}}{\mathrm{d}t}\|d^p\|^2 + \epsilon^2\|d^\chi\|^2 = (\phi\, d^\chi, d^p) \le C_\phi\|d^\chi\|\|d^p\|,$$

or, after applying a Young inequality,

$$\frac{\mathrm{d}}{\mathrm{d}t}\|d^p(t)\|^2 + \epsilon^2\|d^\chi\|^2 \le C_\phi\epsilon^{-2}\|d^p\|^2.$$

Since $d^p(0) = 0$, the application of a Gronwall inequality yields $\|d^p(t)\|^2 = 0$ for a.e. $t \in [0, T]$ and subsequently $\int_0^T \|d^\chi\|^2\, \mathrm{d}t = 0$. This completes the proof of Theorem 5.A.

VI. NUMERICAL RESULTS

In the following numerical experiments, we investigate the convergence of the dual-based error estimate, $\mathrm{Est}(\hat{u}, \hat{\mu}; \hat{p}, \hat{\chi})$ in (40), under uniform refinements in space and time. We compare this with the convergence of the true error. A useful measure of the performance of the estimate is the effectivity, which is defined as the ratio of the error estimate to the true error:

$$\text{Effectivity} = \frac{\mathrm{Est}(\hat{u}, \hat{\mu}; \hat{p}, \hat{\chi})}{\mathcal{Q}(u, \mu) - \mathcal{Q}(\hat{u}, \hat{\mu})}.$$

Ideally, the effectivity equals one. Let us first describe how fully discrete approximations $(\hat{u}, \hat{\mu})$ and $(\hat{p}, \hat{\chi})$ are computed.

A. Fully-Discrete Semi-Implicit Schemes

We obtain fully discrete approximations $(\hat{u}, \hat{\mu})$ by applying a semi-implicit time-stepping algorithm to (9) following ideas in [18,23]. The semi-implicit scheme employs a splitting of the free energy into a convex and concave part,

$$\psi(u) = \psi_c(u) - \psi_e(u),$$

where ψ_c and ψ_e are both convex functions also referred to as the contractive and expansive part, respectively. For the free energy function ψ in (2), this (nonunique) splitting can be chosen as

$$\psi_c(u) := \alpha\, u^2, \quad \psi_e(u) := \psi_c(u) - \psi(u),$$

for any $\alpha \ge 1$. We shall use $\alpha = 1.5$ in the sequel.

We consider lowest-order in space approximations based on $S^{h,1} := S^{h,1}(\mathcal{P}^h)$ (i.e., linear finite elements). For constant time steps the fully discrete scheme is defined recursively by

$$\text{Find } (u^{n+1}, \mu^{n+1}) \in S^{h,1} \times S^{h,1} :$$

$$\Big(\frac{u^{n+1} - u^n}{\Delta t}, v\Big) + (\nabla \mu^{n+1}, \nabla v) = 0 \qquad \forall v \in S^{h,1}, \tag{50a}$$

$$-\epsilon^2 (\nabla u^{n+1}, \nabla \eta) + \big(-\psi_c'(u^{n+1}) + \psi_e'(u^n) + \mu^{n+1}, \eta\big) = 0 \qquad \forall \eta \in S^{h,1}, \tag{50b}$$

for $n = 0, \ldots, N-1$, where the initial condition $u^0 \in S^{h,1}$ is defined by

$$(u^0, w) = (u_0, w) \quad \forall w \in S^{h,1}. \tag{50c}$$

Subsequently, the approximation $(\hat{u}, \hat{\mu})$ is defined for all $t \in [0, T]$ using linear interpolation:

$$\left.\begin{aligned} \hat{u}(t) &= \frac{t - t^n}{\Delta t} u^{n+1} + \frac{t^{n+1} - t}{\Delta t} u^n \\ \hat{\mu}(t) &= \frac{t - t^n}{\Delta t} \mu^{n+1} + \frac{t^{n+1} - t}{\Delta t} \mu^n \end{aligned}\right\} \quad t \in [t^n, t^{n+1}]. \tag{51}$$

An important stability result for the scheme above, mimicking (5) on the discrete level, is the following.

Proposition 6.1 (gradient-stability). *The fully discrete scheme* (50) *is gradient-* (*or energy-*) *stable, in that it satisfies*

$$\mathcal{E}(u^{n+1}) - \mathcal{E}(u^n) \leq -\Delta t \int_\Omega |\nabla \mu^{n+1}| \, \mathrm{d}x \qquad \forall n = 0, \ldots, N-1.$$

Proof. The proof follows as in Section 2.1 of [23]. ∎

Remark 6.2. Since $\psi(u)$ in (2) has quadratic growth as $u \to \infty$ it is possible to select a quadratic ψ_c, unlike for a pure quartic free energy (requiring, in principle, a quartic ψ_c for a valid splitting). The advantage of a quadratic ψ_c is that the corresponding semi-implicit scheme (50) requires the solution of a linear system at each time step.

To discretize the dual problem (34), we consider higher-order in space approximations based on $S^{h,2} := S^{h,2}(\mathcal{P}^h)$ (i.e., quadratic finite elements)[7] in conjunction with a semi-implicit time-stepping scheme:

$$\text{Find } (p^n, \chi^n) \in S^{h,2} \times S^{h,2} :$$

$$-\Big(\frac{p^{n+1} - p^n}{\Delta t}, v\Big) - \epsilon^2 (\nabla \chi^n, \nabla v) - \big(\psi_c''(u^{n+1})\chi^n - \psi_e''(u^{n+1})\chi^{n+1}, v\big) = \big(q_1(t^n), v\big) \qquad \forall v \in S^{h,2}, \tag{52a}$$

$$(\nabla p^n, \nabla \eta) + (\chi^n, \eta) = \big(q_2(t^n), \eta\big) \qquad \forall \eta \in S^{h,2}, \tag{52b}$$

[7] It is well known [45] that using the same approximation in space for the dual problem renders the dual-based error estimate useless owing to Galerkin orthogonality, cf. Corollary 4.2.

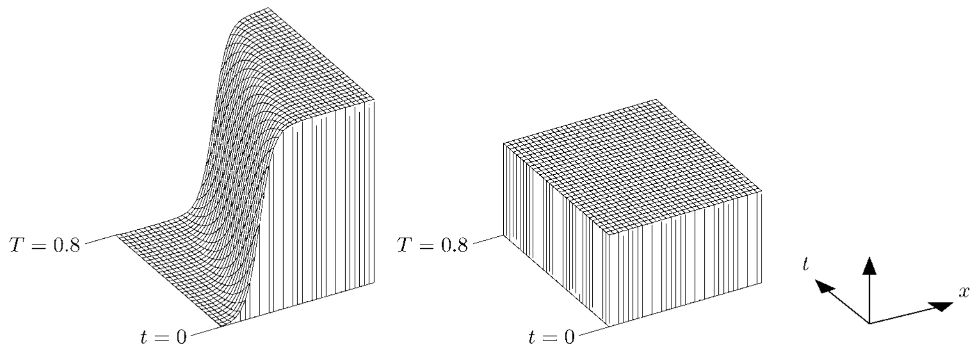

FIG. 1. 1-D propagating front test case. The primal solutions u (left) and μ (right).

for $n = N-1, N-2, \ldots, 1, 0$. Note that the scheme marches backward in time, starting from the "initial" condition $p^N \in S^{h,2}$ defined by

$$(p^N, w) = (\bar{q}, w) \qquad \forall w \in S^{h,2}, \tag{52c}$$

Similar to (51), we obtain an approximation $(\hat{p}, \hat{\chi})$ for all $t \in [0, T]$ using linear interpolation.

B. 1-D Propagating Front

In the first test-case, we consider the Cahn–Hilliard equation in 1-D. Inspired by [36], we impose as a solution the following (manufactured) propagating front:

$$\tilde{u}(x,t) = \tanh\left(\frac{x - 0.5t - 0.25}{\sqrt{2}\,\epsilon}\right).$$

For each time t, $\tilde{u}(x,t)$ actually satisfies the time-independent Cahn–Hilliard equation on $\mathbb{R}$ ($\tilde{u}(x,t)$ is a so-called transition solution with $\psi'(\tilde{u}) - \epsilon^2\,\Delta\tilde{u} = 0$). For the time-dependent case, this means that we have a source term f on the right-hand side of $(1a)_1$:

$$f(x,t) = \tilde{u}_t(x,t),$$

and a nonhomogeneous Neumann boundary condition, both of which can easily be included in the error analyses in the paper. We take $\epsilon = 1/16 = 0.0625$, $\Omega = (0,1)$ and the final time $T = 0.8$. The solution corresponding to these parameters is depicted in Fig. 1.

As the quantity of interest, we take $q_1 = q_2 = 0$ and $\bar{q}$ as a C^1-continuous, piecewise quadratic polynomial with width, maximum and center of 0.25, 1.0 and 0.625, respectively. The exact value of the quantity of interest is

$$\mathcal{Q}(u,\mu) = (\bar{q}, u(0.8)) = -0.028829294\ldots.$$

Figure 2 displays a fine solution of the dual solution corresponding to $\mathcal{Q}$. Note that the dual solution exhibits exponential decay. We believe that the reason for this is that the dual problem has been obtained by linearizing at an approximation with developed layers.

The convergence of the error $\mathcal{Q}(u,\mu) - \mathcal{Q}(\hat{u},\hat{\mu})$ and the dual-based error estimate $\text{Est}(\hat{u},\hat{\mu};\hat{p},\hat{\chi})$ with respect to uniform refinements in space and time is depicted in Table I.

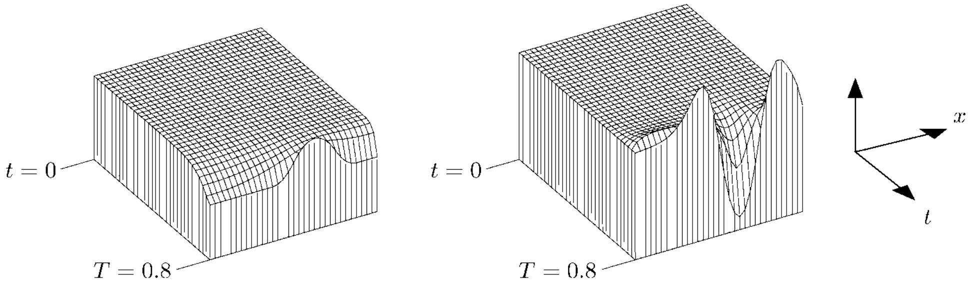

FIG. 2. 1-D propagating front test case. Computed dual solutions $\hat{p}$ (left) and $\hat{\chi}$ (right), which are solved backward in time from $t = T$ to $t = 0$.

We have also displayed the effectivity. From these results, it can be seen that the time discretization dominates the error. Note that the effectivity converges to one under space–time refinement, demonstrating the consistency and accuracy of the error estimate.

To investigate the accuracy of the error estimate with respect to ϵ, we perform the same numerical experiment for ϵ twice as large and twice as small; see Table II. From these results it is visible that for smaller ϵ (sharper fronts), one requires a finer discretization to have similar accuracy of the error estimate. The precise relation, however, is not completely clear from the results.

C. 1-D Spinodal Decomposition

In the next numerical experiment, we consider spinodal decomposition in 1-D on the domain $\Omega = (0, 1)$. We impose an initial condition u_0 within the spinodal regime:

$$u_0(x) = \frac{3}{10}(1 - 2x).$$

TABLE I. 1-D propagating front test case.

	$\mathcal{Q}(u,\mu) - \mathcal{Q}(\hat{u},\hat{\mu})$			$\mathrm{Est}(\hat{u},\hat{\mu};\hat{p},\hat{\chi})$			Effectivity		
# Elems	$N = 32$	64	128	32	64	128	32	64	128
8	−0.04558	−0.02575	−0.01310	−0.03388	−0.02521	−0.01560	0.743	0.979	1.191
16	−0.05104	−0.02617	−0.01315	−0.04242	−0.02574	−0.01330	0.831	0.984	1.011
32	−0.05348	−0.02755	−0.01373	−0.04431	−0.02715	−0.01387	0.829	0.986	1.010
64	−0.05414	−0.02794	−0.01391	−0.04479	−0.02751	−0.01403	0.827	0.985	1.009
128	−0.05431	−0.02804	−0.01396	−0.04491	−0.02760	−0.01407	0.827	0.984	1.008

Convergence of the error, estimate, and effectivity with respect to spatial and temporal refinement.

TABLE II. 1-D propagating front test case.

	$\epsilon = 1/8$			$\epsilon = 1/16$			$\epsilon = 1/32$		
# Elems	$N = 32$	64	128	32	64	128	32	64	128
8	0.909	1.029	1.157	0.743	0.979	1.191	0.420	0.912	1.632
16	0.922	0.991	1.033	0.831	0.984	1.011	0.406	1.046	1.262
32	0.925	0.984	1.004	0.829	0.986	1.010	0.331	0.940	1.104
64	0.925	0.982	0.997	0.827	0.985	1.009	0.307	0.902	1.041
128	0.926	0.981	0.995	0.827	0.984	1.008	0.301	0.892	1.024

Convergence of the effectivity with respect to spatial and temporal refinement for various ϵ.

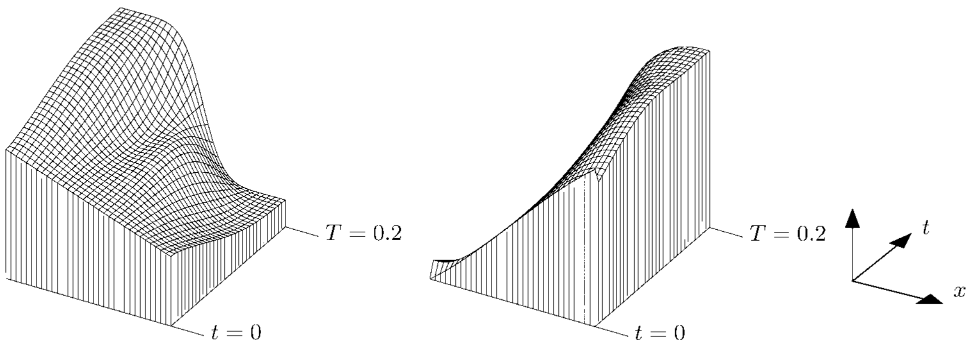

FIG. 3. 1-D spinodal decomposition test case. Approximations to the solution u (left) and μ (right) solved with large time steps.

Furthermore, we take $\epsilon = 1/16 = 0.0625$ and $T = 0.2$. For this initial condition, we expect the solution to asymptotically evolve toward a steady-state transition solution.

In the numerical experiments, the time discretization again dominates the accuracy of approximations. In particular, if the time-step size is too large, then the approximation evolves quickly to the final transition solution. Such an approximation is visible in Fig. 3 which has been obtained with 64 time steps. However, if the time-step size is small enough, it is actually visible that the solution passes through a meta-stable state; see Fig. 4 obtained with 256 time steps. This qualitatively different behavior can also be observed in Fig. 5, which shows the total free energy evolution $t \mapsto \mathcal{E}(\hat{u}(t))$ corresponding to these two simulations. Note that at time $T = 0.2$ the approximations are in different (meta-) stable states.

We consider the same quantity of interest as for the propagating front test case, i.e., $q_1 = q_2 = 0$ and $\bar{q}$ is a C^1-continuous, piecewise quadratic polynomial. Since we do not have an exact solution, we compute a reference value for $\mathcal{Q}$ using 512 spatial elements, and extrapolate the values obtained with 4,096 and 8,192 time steps (anticipating $O(\Delta t)$ convergence), yielding

$$\mathcal{Q}(u, \mu) = (\bar{q}, u(0.2)) \approx 0.08826.$$

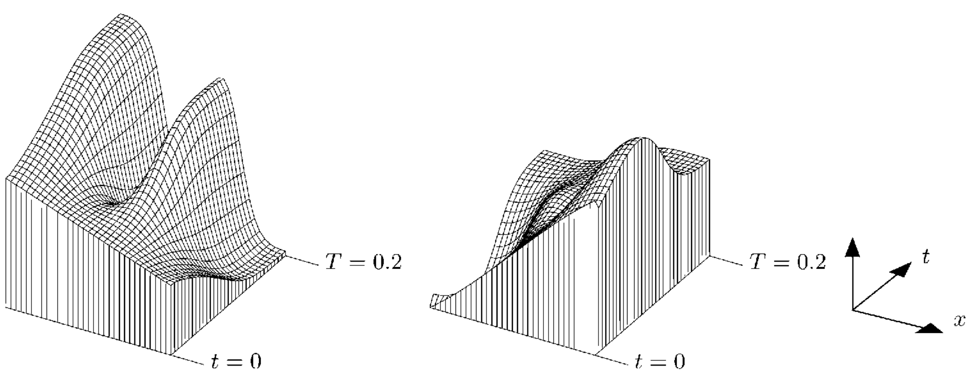

FIG. 4. 1-D spinodal decomposition test case. Approximations to the solution u (left) and μ (right) solved using sufficiently small time steps.

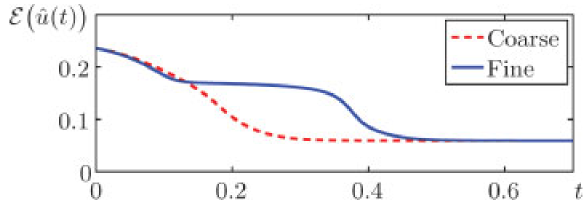

FIG. 5. 1-D spinodal decomposition test case. Total free energy evolution corresponding to a coarse approximation (- - -) with large time steps (see Fig. 3) and a fine approximation (—) with small time steps (see Fig. 4). [Color figure can be viewed in the online issue, which is available at wileyonlinelibrary.com.]

A computed dual solution, corresponding to the small time-step approximation in Fig. 4, is shown in Fig. 6. Note that half-way into the simulation time, it grows exponentially fast (although it does not blow up in finite time). This is expected, since (going backward in time) we encounter the situation that the forward approximation is in the spinodal (unstable) regime. Note that this is in accordance with the estimate derived in Theorem 5.A. In Table III we show the convergence of the error estimate with respect to temporal refinement for a sufficiently fine uniform mesh (128 elements). For large time steps, the quantity of interest is completely incorrect having the wrong sign. This is reflected in the accuracy of the estimate. However, if the evolution is qualitatively captured (at least 256 time steps), the estimate is accurate. Note that the effectivity converges again to one indicating the asymptotic exactness of the estimate.

D. Merging Bubbles

In the last numerical experiment, we consider a two-dimensional test case similar to the first numerical experiment in [32]. It involves the merging of a small bubble of size 0.25 with a large bubble of size 0.3 in the domain $\Omega = (0, 1) \times (0, 1)$. The initial condition is given by

$$u_0(x, y) = \tanh(((x - 0.3)^2 + y^2 - 0.25^2)/\epsilon)\ \tanh(((x + 0.3)^2 + y^2 - 0.3^2)/\epsilon),$$

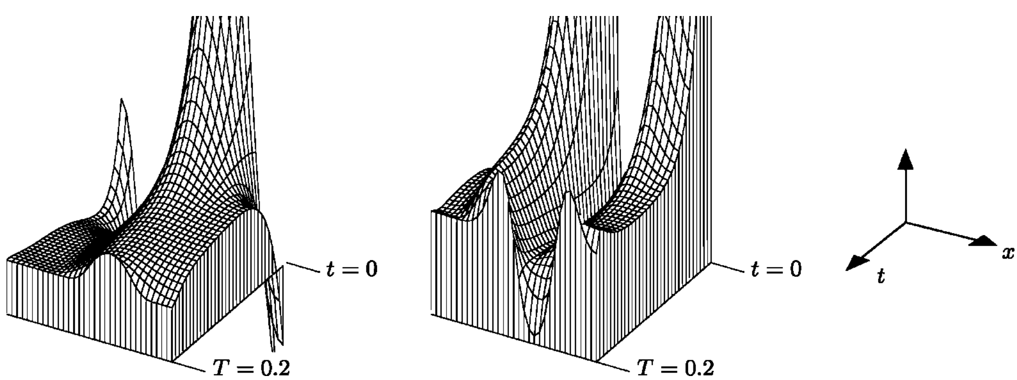

FIG. 6. 1-D spinodal decomposition test case. Computed dual solutions $\hat{p}$ (left) and $\hat{\chi}$ (right) corresponding to the forward approximation $(\hat{u}, \hat{\mu})$ visible in Fig. 4. Note that the dual problem is solved backward in time from $t = T$ to $t = 0$.

TABLE III. 1-D spinodal decomposition test case.

N	$\mathcal{Q}(\hat{u}, \hat{\mu})$	$\mathcal{Q}(u, \mu) - \mathcal{Q}(\hat{u}, \hat{\mu})$	$\text{Est}(\hat{u}, \hat{\mu}; \hat{p}, \hat{\chi})$	Effectivity
16	−0.08540	0.17366	−0.03654	−0.210
32	−0.11169	0.19995	−0.02857	−0.143
64	−0.11829	0.20656	0.02218	0.107
128	−0.00008	0.08834	0.22182	2.511
256	0.06385	0.02441	0.03368	1.380
512	0.07792	0.01034	0.01178	1.139
1,024	0.08340	0.00487	0.00517	1.062
2,048	0.08587	0.00240	0.00247	1.029

Convergence of the quantity of interest, error, estimate, and effectivity with respect to temporal refinement (using 128 spatial elements).

see Fig. 7. The total simulation time is $T = 2.0$, and we set $\epsilon = 0.08$. In Fig. 8, several snapshots are visible of the approximation obtained on a uniform triangular mesh with 4,096 elements and 64 time steps.

We are interested in the x-coordinate of the center of volume of the merged bubble at the final time:

$$x_c(T) := \frac{1}{V} \int_\Omega \frac{1}{2}(1 - u(T, x, y))\, x \, \mathrm{d}x \, \mathrm{d}y,$$

where the total volume V (constant during the simulation) is given as

$$V := \int_\Omega \frac{1}{2}(1 - u(T, x, y)) \, \mathrm{d}x \, \mathrm{d}y = \int_\Omega \frac{1}{2}(1 - u_0(x, y)) \, \mathrm{d}x \, \mathrm{d}y.$$

To calculate $x_c(T)$, we thus consider the following quantity of interest:

$$\mathcal{Q}(u, \mu) = -\int_\Omega \frac{1}{2}\, u(T, x, y)\, x \, \mathrm{d}x \, \mathrm{d}y,$$

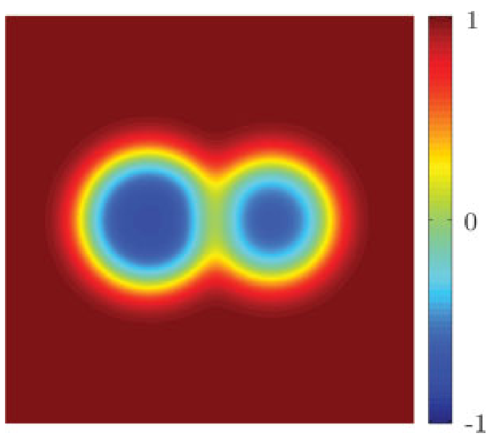

FIG. 7. Merging bubbles test case. The initial condition for u. [Color figure can be viewed in the online issue, which is available at wileyonlinelibrary.com.]

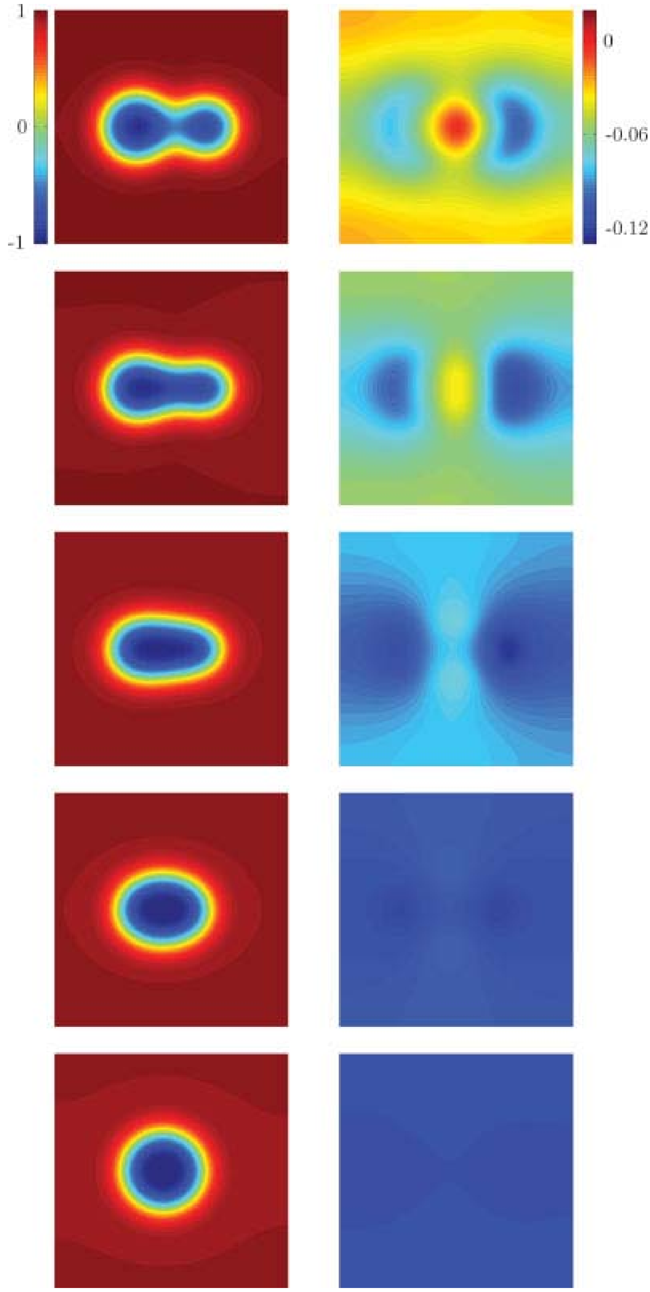

FIG. 8. Merging bubbles test case. From top to bottom: computed solution $\hat{u}$ (left) and $\hat{\mu}$ (right) at time 0.125, 0.25, 0.5, 1.0, and 2.0 (final time). [Color figure can be viewed in the online issue, which is available at wileyonlinelibrary.com.]

which corresponds to $\mathcal{Q}$ in (24) with $q_1 = q_2 = 0$ and $\bar{q}(x, y) = -\frac{1}{2}x$. To have a reference value for this quantity of interest, we solve the forward problem on a uniform mesh with 262,144 elements and extrapolate (anticipating $O(\Delta t)$ convergence) the values obtained using 8,192 and 16,384 time steps, resulting in:

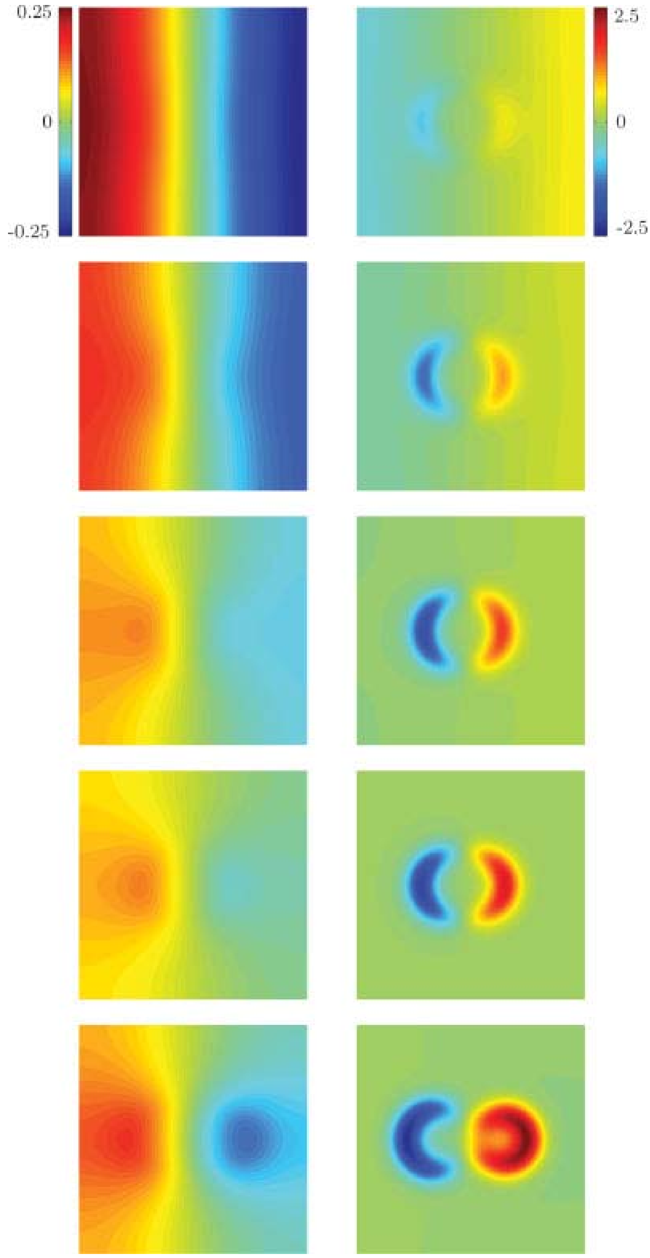

FIG. 9. Merging bubbles test case. From top to bottom: computed dual solutions $\hat{p}$ (left) and $\hat{\chi}$ (right) at time 1.9375, 1.875, 1.5, 1.0, and 0.0 (initial forward time). Note that the dual solution is solved backward in time. [Color figure can be viewed in the online issue, which is available at wileyonlinelibrary.com.]

$$\mathcal{Q}(u, \mu) \approx -0.02407.$$

Several snapshots of a computed dual solution, corresponding to the forward approximation in Fig. 8, are visible in Fig. 9. Note that $\hat{p}$ (starting off from $\bar{q}$) initially exhibits decay, with growth

TABLE IV. Merging bubbles test case.

# Elems	$\mathcal{Q}(u,\mu)-\mathcal{Q}(\hat{u},\hat{\mu})$ $N=64$	256	1,024	$\mathrm{Est}(\hat{u},\hat{\mu};\hat{p},\hat{\chi})$ 64	256	1,024	Effectivity 64	256	1,024
64	−0.01183	−0.02205	−0.02306	−0.26392	−1.78933	−7.76063	22.311	81.162	336.469
256	0.00946	0.01751	0.01982	0.02108	0.12233	0.38726	2.229	6.985	19.537
1,024	0.00199	0.00104	0.00073	0.00322	0.00362	0.00315	1.620	3.484	4.308
4,096	0.00165	0.00049	0.00012	0.00173	0.00077	0.00021	1.045	1.572	1.774
16,384	0.00162	0.00048	0.00011	0.00144	0.00055	0.00013	0.886	1.146	1.159

Convergence of the error, estimate, and effectivity with respect to spatial and temporal refinement.

toward the end. The dual approximation $\hat{\chi}$ (starting off from 0) grows throughout the simulation. This growth is localized at the interface of the merging bubbles. Table IV shows the convergence of the error estimate with respect to space–time refinement. Extremely coarse meshes fail to resolve the interfaces, which is reflected in the accuracy of the estimates. However, for qualitatively resolved interfaces, the estimate is accurate, even for large time steps, and asymptotically exact.

VII. CONCLUDING REMARKS

We have provided an analysis of a posteriori estimates of errors for a class of quantities of interest for initial-boundary-value problems governed by the Cahn–Hilliard equations. This entailed a study of the backward-in-time adjoint problem, for which we established existence and uniqueness results and results on well posedness. We explored mixed finite element approximations of this system and derived estimates of error bounds in the form of computable approximations of residual functionals. The results of several numerical experiments on one- and two-dimensional examples indicate good performance and accuracy of the error estimates provided the dynamics and layers are qualitatively resolved. Effectivity indices approach unity as the mesh size and time step are appropriately reduced.

The authors thank Regina Almeida for useful discussions on numerical algorithms for the Cahn–Hilliard equation.

References

1. J. W. Cahn and J. E. Hilliard, Free energy of a nonuniform system. I. Interfacial free energy, J Chem Phys 28 (1958), 258–267.
2. D. M. Anderson, G. B. McFadden, and A. A. Wheeler, Diffuse-interface methods in fluid mechanics, Annu Rev Fluid Mech 30 (1998), 139–165.
3. J. S. Lowengrub and L. Truskinovsky, Quasi-incompressible Cahn–Hilliard fluids and topological transitions, Proc R Soc Lond Ser A Math Phys Eng Sci 454 (1998), 2617–2654.
4. W. J. Boettinger, J. A. Warren, C. Beckermann, and A. Karma, Phase-field simulation of solidification, Annu Rev Mater Res 32 (2002), 163–194.
5. L.-Q. Chen, Phase-field models for microstructure evolution, Annu Rev Mater Res 32 (2002), 113–140.
6. J. Oden, A. Hawkins, and S. Prudhomme, General diffuse-interface theories and an approach to predictive tumor growth modeling, Math Models Methods Appl Sci 20 (2010), 477–517.
7. C. Elliott and S. Zheng, On the Cahn–Hilliard equation, Arch Ration Mech Anal 96 (1986), 339–357.

8. C. Elliott, The Cahn–Hilliard model for the kinetics of phase separation, J. Rodrigues, editor, Mathematical Models for phase change problems: Proceedings of the European Workshop held at Óbidos, Portugal, October 1-3, 1988, Vol. 88: International Series of Numerical Mathematics, Birkhäuser, Basel, 1989, pp. 35–73.

9. J. Blowey and C. Elliott, The Cahn–Hilliard gradient theory for phase separation with non-smooth free energy. Part I: Mathematical analysis, European J Appl Math 2 (1991), 233–279.

10. C. M. Elliott and S. Luckhaus, A generalized equation for phase separation of a multi-component mixture with interfacial free energy, IMA Preprint Series 887, Institute for Mathematics and its Applications, University of Minnesota, Minneapolis, Minnesota, 1991.

11. C. Elliott and H. Garcke, On the Cahn–Hilliard equation with degenerate mobility, SIAM J Math Anal 27 (1996), 404–423.

12. J. Barrett and J. Blowey, Finite element approximation of the Cahn–Hilliard equation with concentration dependent mobility, Math Comp 68 (1999), 487–517.

13. B. Nicolaenko, B. Scheurer, and R. Temam, Some global dynamical properties of a class of pattern formation equations, Comm Partial Differential Equations (1989), 245–297.

14. R. L. Pego, Front migration in the nonlinear Cahn–Hilliard equation, Proc. R. Soc. Lond. Ser. A Math. Phys. Eng. Sci. 422 (1989), 261–278.

15. N. D. Alikakos, P. W. Bates, and X. Chen, Convergence of the Cahn–Hilliard equation to the Hele–Shaw model, Arch Ration Mech Anal 128 (1994), 165–205.

16. X. Chen, Global asymptotic limit of solutions of the Cahn–Hilliard equation, J Differential Geom 44 (1996), 262–311.

17. M. Burger, S.-Y. Chu, P. A. Markowich, and C.-B. Schönlieb, The Willmore functional and instabilities in the Cahn–Hilliard equation, Commun Math Sci 6 (2008), 309–329.

18. D. Eyre, Unconditionally gradient stable time marching the Cahn–Hilliard equation, J. W. Bullard, L.-Q. Chen, R. K. Kalia, and A. M. Stoneham, editors, Computational and mathematical models of microstructural evolution, Vol. 529: Materials Research Society Symposium Proceedings, Materials Research Society, Warrendale, PA, 1998, pp. 39–46.

19. Y. He, Y. Liu, and T. Tang, On large time-stepping methods for the Cahn–Hilliard equation, Appl. Numer Math 57 (2007), 616–628.

20. L. He and Y. Liu, A class of stable spectral methods for the Cahn–Hilliard equation, J Comput Phys 228 (2009), 5101–5110.

21. X. Feng and A. Prohl, Numerical analysis of the Cahn–Hilliard equation and approximation for the Hele–Shaw problem. Part I: Error analysis under minimum regularities, IMA Preprint Series 1798, Institute for Mathematics and its Applications, University of Minnesota, Minneapolis, Minnesota, 2001 Revised version published as [43].

22. C. Xu and T. Tang, Stability analysis of large time-stepping methods for epitaxial growth models, SIAM J Numer Anal 44 (2006), 1759–1779.

23. S. M. Wise, C. Wang, and J. S. Lowengrub, An energy-stable and convergent finite-difference scheme for the phase field crystal equation, SIAM J Numer Anal 47 (2009), 2269–2288.

24. C. Elliott and D. French, Numerical studies of the Cahn–Hilliard equation for phase separation, IMA J Appl Math 38 (1987), 97–128.

25. M. Copetti and C. Elliott, Numerical analysis of the Cahn–Hilliard equation with a logarithmic free energy, Numer Math 63 (1992), 39–65.

26. J. Barrett and J. Blowey, An error bound for the finite element approximation of the Cahn–Hilliard equation with logarithmic free energy, Numer Math 72 (1995), 1–20.

27. X. Feng and A. Prohl, Error analysis of a mixed finite element method for the Cahn–Hilliard equation, Numer Math 99 (2004), 47–84.

28. G. N. Wells, E. Kuhl, and K. Garikipati, A discontinuous Galerkin method for the Cahn–Hilliard equation, J Comput Phys 218 (2006), 860–877.

29. X. Feng and O. A. Karakashian, Fully discrete dynamic mesh discontinuous Galerkin methods for the Cahn–Hilliard equation of phase transition, Math Comp 76 (2007), 1093–1117.

30. D. Kay, V. Styles, and E. Süli, Discontinuous Galerkin finite element approximation of the Cahn–Hilliard equation with convection, SIAM J Numer Anal 47 (2009), 2660–2685.

31. H. Gómez, V. M. Calo, Y. Bazilevs, and T. J. R. Hughes, Isogeometric analysis of the Cahn–Hilliard phase-field model, Comput Methods Appl Mech Engrg 197 (2008), 4333–4352.

32. X. Feng and H.-J. Wu, A posteriori error estimates for finite element approximations of the Cahn–Hilliard equation and the Hele–Shaw flow, J Comput Math 26 (2008), 767–796.

33. S. Bartels and R. Müller, A posteriori error controlled local resolution of evolving interfaces for generalized Cahn–Hilliard equations, Interfaces Free Bound 12 (2010), 45–73.

34. L. Baňas and R. Nürnberg, Adaptive finite element methods for Cahn–Hilliard equations, J Comput Appl Math 218 (2008), 2–11.

35. L. Baňas and R. Nürnberg, A posteriori estimates for the Cahn–Hilliard equation with obstacle free energy, M2AN Math Model Numer Anal 43 (2009), 1003–1026.

36. D. Kessler, R. H. Nochetto, and A. Schmidt, A posteriori error control for the Allen–Cahn problem: Circumventing Gronwall's inequality, M2AN Math Model Numer Anal 38 (2004), 129–142.

37. S. Bartels, A posteriori error analysis for time-dependent Ginzburg–Landau type equations, Numer Math 99 (2005), 557–583.

38. X. Feng and H.-J. Wu, A posteriori error estimates and an adaptive finite element method for the Allen–Cahn equation and the mean curvature flow, J Sci Comput 24 (2005), 121–146.

39. S. Prudhomme and J. T. Oden, On goal-oriented error estimation for elliptic problems: application to the control of pointwise errors, Comput Methods Appl Mech Engrg 176 (1999), 313–331.

40. J. T. Oden and S. Prudhomme, Goal-oriented error estimation and adaptivity for the finite element method, Comput Math Appl 41 (2001), 735–756.

41. J. T. Oden and S. Prudhomme, Estimation of modeling error in computational mechanics, J Comput Phys 182 (2002), 496–515.

42. S. Prudhomme and J. T. Oden, Computable error estimators and adaptive techniques for fluid flow problems, T. J. Barth and H. Deconinck, editors, Error estimation and adaptive discretization methods in computational fluid dynamics, Vol. 25: Lecture Notes in Computational Science and Engineering, Springer-Verlag, Heidelberg, 2003, pp. 207–268.

43. R. Becker and R. Rannacher, A feed-back approach to error control in finite element methods: Basic analysis and examples, East-West J Numer Math 4 (1996), 237–264.

44. R. Becker and R. Rannacher, An optimal control approach to a posteriori error estimation in finite element methods, Acta Numer 10 (2001), 1–102.

45. W. Bangerth and R. Rannacher, Adaptive Finite Element Methods for Differential Equations, Lectures in Mathematics, ETH Zürich, Birkhäuser, 2003.

46. P. Houston and E. Süli, hp-adaptive discontinuous Galerkin finite element methods for first-order hyperbolic problems, SIAM J Sci Comput 23 (2001), 1226–1252.

47. E. Süli and P. Houston, Adaptive finite element approximation of hyperbolic problems, T. J. Barth and H. Deconinck, editors, Error estimation and adaptive discretization methods in computational fluid dynamics, Vol. 25: Lecture Notes in Computational Science and Engineering, Springer-Verlag, Heidelberg, 2003, pp. 269–344.

48. M. Paraschivoiu, J. Peraire, and A. T. Patera, A posteriori finite element bounds for linear-functional outputs of elliptic partial differential equations, Comput Methods Appl Mech Engrg 150 (1997), 289–312.

49. A. T. Patera and J. Peraire, A general Lagrangian formulation for the computation of a posteriori finite element bounds, T. J. Barth and H. Deconinck, editors, Error Estimation and Adaptive Discretization Methods in Computational Fluid Dynamics, Vol. 25: Lecture Notes in Computational Science and Engineering, Springer-Verlag, Heidelberg, 2003, pp. 159–206.

50. W. Bangerth and R. Rannacher, Finite element approximation of the acoustic wave equation: Error control and mesh adaptation, East-West J Numer Math 7 (1999), 263–282.

51. D. Fuentes, D. Littlefield, J. T. Oden, and S. Prudhomme, Extensions of goal-oriented error estimation methods to simulations of highly-nonlinear response of shock-loaded elastomer-reinforced structures, Comput Methods Appl Mech Engrg 195 (2006), 4659–4680.

52. P. Díez and G. Calderón, Goal-oriented error estimation for transient parabolic problems, Comput Mech 39 (2007), 631–646.

53. M. Schmich and B. Vexler, Adaptivity with dynamic meshes for space–time finite element discretization of parabolic equations, SIAM J Sci Comput 30 (2008), 369–393.

54. R. Bermejo and J. Carpio, A space–time adaptive finite element algorithm based on dual weighted residual methodology for parabolic equations, SIAM J Sci Comput 31 (2009), 3324–3355.

55. V. Carey, D. Estep, A. Johansson, M. Larson, and S. Taverner, Blockwise adaptivity for time dependent problems based on coarse scale adjoint solutions, Technical Report, Department of Mathematics, Colorado State University, Fort Collins, Colorado, 2009.

56. K. Eriksson and C. Johnson, Adaptive finite element methods for parabolic problems I: A linear model problem, SIAM J Numer Anal 28 (1991), 43–77.

57. K. Eriksson and C. Johnson, Adaptive finite element methods for parabolic problems II: Optimal error estimates in $L_\infty L_2$ and $L_\infty L_\infty$, SIAM J Numer Anal 32 (1993), 706–740.

58. K. Eriksson and C. Johnson, Adaptive finite element methods for parabolic problems IV: Nonlinear problems, SIAM J Numer Anal 32 (1995), 1729–1749.

59. K. Eriksson and C. Johnson, Adaptive finite element methods for parabolic problems V: Long-time integration, SIAM J Numer Anal 32 (1995), 1750–1763.

60. K. Eriksson, D. Estep, P. Hansbo, and C. Johnson, Computational Differential Equations, Cambridge University Press, Cambridge, 1996.

61. K. Eriksson, C. Johnson, and A. Logg, Adaptive computational methods for parabolic problems, E. Stein, R. de Borst, and T. J. R. Hughes, editors, Encyclopedia of computational mechanics, Vol. 1: Fundamentals, chapter 24, John Wiley & Sons, N.Y., 2004, pp. 675–702.

62. L. A. Caffarelli and N. E. Muler, An L^∞ bound for solutions of the Cahn–Hilliard equation, Arch Ration Mech Anal 133 (1995), 129–144.

63. P. Fife, Models for phase separation and their mathematics, Electron J Differential Equations 48 (2000), 1–26.

64. L. Evans, Partial Differential Equations, Vol. 19: Graduate Studies in Mathematics, American Mathematical Society, Providence, 1998.

65. R. Dautray and J.-L. Lions, Mathematical analysis and numerical methods for science and technology. Vol. 5: Evolution Problems I, Springer-Verlag, Berlin, 1992.

66. P. G. Ciarlet and P.-A. Raviart, A mixed finite element method for the biharmonic equation, C. de Boor, editor, Mathematical Aspects of Finite Elements in Partial Differential Equations, Academic Press, New York, 1974, pp. 125–145. Proceedings of the Symposium on Mathematical Aspects of Finite Elements in Partial Differential Equations held in Madison, Wisconsin, April 1–3, 1974.

67. P. G. Ciarlet, The Finite Element Method for Elliptic Problems, Vol. 40: Classics in Applied Mathematics, SIAM, Society for Industrial and Applied Mathematics, Philadelphia, SIAM ed., 2002. First published by North-Holland, 1978.

68. M. B. Giles and E. Süli, Adjoint methods for PDEs: A posteriori error analysis and postprocessing by duality, Acta Numer (2002), 145–236.

69. E. Bänsch and K. G. Siebert, A posteriori error estimation for nonlinear problems by duality techniques, Technical Report, Institut für Angewandte Mathematik, Albert-Ludwigs-Universität Freiburg, Freiburg, Germany, 1995.

70. K. G. van der Zee, E. H. van Brummelen, and R. de Borst, Goal-oriented error estimation and adaptivity for free-boundary problems: The domain-map linearization approach, SIAM J Sci Comput 32 (2010), 1064–1092.

71. K. G. van der Zee, E. H. van Brummelen, and R. de Borst, Goal-oriented error estimation and adaptivity for free-boundary problems: The shape linearization approach, SIAM J Sci Comput 32 (2010), 1093–1118.

72. E. Süli, A posteriori error analysis and adaptivity for finite element approximations of hyperbolic problems, D. Kröner, M. Ohlberger, and C. Rohde, editors, An introduction to recent developments in theory and numerics for conservation laws, Vol. 5: Lecture Notes in Computational Science and Engineering, Springer, Berlin, 1999, pp. 123–194.

73. R. H. Nochetto, A. Schmidt, and C. Verdi, A posteriori error estimation and adaptivity for degenerate parabolic problems, Math Comp 69 (1999), 1–24.

74. J. Lions, Quelques Méthodes de Résolution des Problèmes aux Limites Non Linéaires, Études Mathématiques, Dunod, 1969.

75. S. Zheng, Nonlinear Evolution Equations, Vol. 133: Monographs and surveys in pure and applied mathematics, Chapman & Hall, Boca Raton, 2004.